The differentiation and integration of the hippocampal dorsoventral axis are controlled by two nuclear receptor genes

Xiong Yang[1#], Rong Wan[1#], Zhiwen Liu[2,3], Su Feng[2,3], Jiaxin Yang[1], Naihe Jing[2,3*], Ke Tang[1*]

1, Precise Genome Engineering Center, School of Life Sciences, Guangzhou University, Guangzhou, Guangdong 510006, China

2, Guangzhou Laboratory/Bioland Laboratory, Guangzhou, 510005, China

3, CAS Key Laboratory of Regenerative Biology, Guangdong Provincial Key Laboratory of Stem Cell and Regenerative Medicine, Guangdong Institutes of Biomedicine and Health, Chinese Academy of Sciences, Guangzhou 510530, China.

#, Co-first authors

*, Co-corresponding authors

Correspondence: njing@sibcb.ac.cn or ktang.sc@gmail.com.

Abstract

The hippocampus executes imperative functions from declarative memory to adaptive behaviors associated with cognition and emotion. However, the mechanisms of how morphogenesis and functions along the hippocampal dorsoventral axis are differentiated and integrated are still largely unclear. Here, we show that *COUP-TFI* and *-TFII* genes are distinctively expressed in the dorsal and ventral hippocampus, respectively. The loss of *COUP-TFII* results in ectopic CA1/CA3 domains in the ventral hippocampus. The deficiency of *COUP-TFI* leads to the failed specification of dorsal CA1, among which there are place cells. The deletion of both *COUP-TF* genes causes almost agenesis of the hippocampus with abnormalities of trisynaptic circuit and adult neurogenesis. Moreover, *COUP-TFI*/*-TFII* may cooperate to guarantee appropriate morphogenesis and function of the hippocampus by regulating the *Lhx5-Lhx2* axis. Our findings revealed a novel mechanism that *COUP-TFI* and *COUP-TFII* converge to govern the differentiation and integration of distinct characteristics of the hippocampus in mice.

Keywords

Memory; Hippocampus; *COUP-TF* Gene; Place Cell; Trisynaptic Circuit

36 **Introduction**

37 Memory, including declarative and nondeclarative memory, unifies our mental world to
38 ensure the quality of life for people of all ages, from newborns to elderly individuals
39 (Eichenbaum & Cohen, 2014; Kandel, Dudai, & Mayford, 2014). The pioneering studies of
40 Milner and her colleagues revealed that the hippocampus is required for declarative memory
41 but not nondeclarative memory (Penfield & Milner, 1958; Scoville & Milner, 1957). The
42 discovery of activity-dependent long-term potentiation and place cells provides the
43 neurophysiological basis of hippocampal function (Bliss & Lomo, 1973; O'Keefe &
44 Dostrovsky, 1971). The rodent hippocampus can be divided into the dorsal and ventral
45 domains, corresponding to the posterior and anterior hippocampus in humans, respectively.
46 In recent decades, numerous studies have supported the Moser theory that the hippocampus is
47 a heterogeneous structure with distinct characteristics of gene expression, connectivity, and
48 functions along its dorsoventral axis (Bast, 2007; Fanselow & Dong, 2010; Moser & Moser,
49 1998; Strange, Witter, Lein, & Moser, 2014). The dorsal hippocampus, which connects and
50 shares similar gene expression with the neocortex (Fanselow & Dong, 2010), serves the "cold"
51 cognitive function associated with declarative memory and spatial navigation. The ventral
52 hippocampus, which connects and generates similar gene expression with the amygdala and
53 hypothalamus (Cenquizca & Swanson, 2007; Kishi et al., 2000; Pitkanen, Pikkarainen,
54 Nurminen, & Ylinen, 2000), corresponds to the "hot" affective states related to emotion and
55 anxiety (Fanselow & Dong, 2010; Tyng, Amin, Saad, & Malik, 2017). Nonetheless, to date,
56 the molecular and cellular mechanisms by which the morphogenesis, connectivity, and
57 functions along the dorsoventral axis of the hippocampus are differentiated and integrated are
58 largely unknown.

59 The hippocampus, a medial temporal lobe structure in the adult rodent forebrain, originates
60 from the medial pallium (MP) in the medial line of the early dorsal telencephalon. The

cortical hem (CH), which is located ventrally to the MP, functions as an organizer for hippocampal development (Hebert & Fishell, 2008; Schuurmans & Guillemot, 2002). It has been demonstrated that both extrinsic signals, such as *Wnts* and *Bmps*, and intrinsic factors, including *Emx1*, *Emx2*, *Lef1*, *Lhx2*, and *Lhx5*, are involved in the regulation of early morphogenesis of the hippocampus. As the earliest *Wnt* gene to be exclusively expressed in the cortical hem, *Wnt3a* is required for the genesis of the hippocampus (S. M. Lee, Tole, Grove, & McMahon, 2000); in addition, *Lef1* is downstream of Wnt signaling, and the hippocampus is completely absent in *Lef1-neo/neo* null mutant mice (Galceran, Miyashita-Lin, Devaney, Rubenstein, & Grosschedl, 2000). Wnt signaling is essential for early development of the hippocampus. *Emx1* and *Emx2* are mouse homologs of *Drosophila empty spiracles* (Simeone et al., 1992). Interestingly, the dorsal hippocampus is smaller in an *Emx1* null mutant (Yoshida et al., 1997), while *Emx2* is required for the growth of the hippocampus but not for the specification of hippocampal lineages (Tole, Goudreau, Assimacopoulos, & Grove, 2000). Moreover, *Lhx5*, which encodes a LIM homeobox transcription factor and is specifically expressed in the hippocampal primordium, is necessary for the formation of the hippocampus (Zhao et al., 1999). *Lhx2*, encoding another LIM homeobox transcription factor, is required for the development of both the hippocampus and neocortex (Mangale et al., 2008; Monuki, Porter, & Walsh, 2001). Intriguingly, deficiency of either *Lhx5* or *Lhx2* results in agenesis of the hippocampus, and more particularly, these genes inhibit each other (Hebert & Fishell, 2008; Mangale et al., 2008; Roy, Gonzalez-Gomez, Pierani, Meyer, & Tole, 2014; Zhao et al., 1999), indicating that the *Lhx5* and *Lhx2* genes may generate an essential regulatory axis to ensure the appropriate hippocampal development. Nevertheless, whether there are other intrinsic genes that participate in the regulation of morphogenesis and function of the hippocampus has not been fully elucidated.

COUP-TF genes, including *COUP-TFI* (also known as *NR2F1*) and *COUP-TFII* (also known as *NR2F2*), encode two transcription factor proteins belonging to the nuclear receptor superfamily (Yang, Feng, & Tang, 2017). Mutations of *COUP-TFI* are highly related to neurodevelopmental disorders (NDD), such as intellectual disability (ID) and autism spectrum disorders (ASD) (Bertacchi et al., 2020; Bosch et al., 2014; Contesse, Ayrault, Mantegazza, Studer, & Deschaux, 2019), and mutations of the *COUP-TFII* gene are associated with congenital heart defects (CHD) (High et al., 2016). By using animal models, our studies and others have demonstrated that *COUP-TF* genes participate in the regulation of the development of the central nervous system (Zhang et al., 2020). The *COUP-TFI* plays an essential role in the differentiation of cortical excitatory projection neurons and inhibitory interneurons, the development of the dorsal hippocampus, and cortical arealization (Armentano et al., 2007; Flore et al., 2017; Lodato et al., 2011; C. Zhou et al., 1999; C. Zhou, Tsai, & Tsai, 2001). *COUP-TFII* plays a vital role in the development of the amygdala, hypothalamus, and cerebellum (S. Feng et al., 2017; Kim, Takamoto, Yan, Tsai, & Tsai, 2009; Tang, Rubenstein, Tsai, & Tsai, 2012). Nevertheless, whether and how *COUP-TFI* and/or *COUP-TFII* genes regulate the differentiation and integration of hippocampal morphogenesis, connectivity, and function is still largely unclear.

Here, our data show that *COUP-TFI* and *-TFII* genes are differentially expressed along the dorsoventral axis of the adult hippocampus. The loss of *COUP-TFII* results in ectopic CA1 and CA3 domains in the ventral hippocampus. In addition, the deficiency of *COUP-TFI* leads to not only dysplasia of the dorsal hippocampus but also failed specification and differentiation of the dorsal CA1 pyramidal neuron lineage. Furthermore, the deletion of both genes in the *RXCre*/+; *COUP-TFI*$^{F/F}$; *COUP-TFII*$^{F/F}$ double mutant mouse causes almost agenesis of the hippocampus, accompanied by compromised specification of the CA1, CA3, and dentate gyrus (DG) domains. The components of the trisynaptic circuit are abnormal in

the corresponding single-gene or double-gene mutant model. Moreover, *COUP-TF* genes may cooperate to guarantee the appropriate morphogenesis and function of the hippocampus by regulating the *Lhx5-Lhx2* axis.

Results

Differential expression profiles of *COUP-TFI* and *-TFII* genes along the dorsoventral axis in the developing and adult hippocampus

To investigate the functions of the *COUP-TFI* and *COUP-TFII* genes in the hippocampus, immunofluorescence staining was first performed to examine their expression in adult wild-type mice at postnatal month 1 (1M). In both the coronal and sagittal sections, COUP-TFI exhibited a septal/dorsal high-temporal/ventral low expression pattern along the hippocampus (Figure 1Aa, d, c, f, g, j, m, i, l, and o), and its expression is highest in the dorsal CA1 region (Figure 1Aa, d, c, f, j, and l), where place cells are mainly located (O'Keefe & Conway, 1978; O'Keefe & Dostrovsky, 1971), and the dorsal DG, where there are adult neural stem cells (NSCs) (Gould & Cameron, 1996). However, the expression of COUP-TFII was high in the temporal/ventral hippocampus but was barely detected in the septal/dorsal part of the hippocampus (Figure 1Ab, c, e, f, h, i, k, l, n, and o). The dorsal-high COUP-TFI and ventral-high COUP-TFII expression profiles were further verified in the adult hippocampi by western blotting assays (Figure 1Ap, q). Interestingly, COUP-TFI and -TFII generated complementary expression patterns in the hippocampal primordium with COUP-TFI in the dorsal MP and COUP-TFII in the ventral CH at embryonic days 12.5 (E12.5) and 14.5 (E14.5) (Figure 1—figure supplement 1Aa-f). Additionally, septal/dorsal-high COUP-TFI and temporal/ventral-high COUP-TFII expression patterns were observed at postnatal day 0 (P0) (Figure 1—figure supplement 1Ag-l). The data above revealed that the differential expression patterns of *COUP-TFI* and *-TFII* genes were generated and maintained along the

135 dorsoventral axis in the early hippocampal primordium, the developing and adult
136 hippocampus, indicating that they could play distinct roles in the mediation of the
137 morphogenesis and functions of the hippocampus.

138 Next, to investigate the roles of *COUP-TF* genes in the hippocampus, an *RXCre* mouse was
139 used to excise the expression of the *COUP-TFI* and/or *COUP-TFII* genes in the hippocampal
140 regions. The deletion efficiency of *RXCre* recombinase was verified by immunofluorescence
141 assays. Compared with control mice, either *COUP-TFII* or *COUP-TFI* could be excised in
142 the adult hippocampus of corresponding single-gene mutants at 1M (Figure 1—figure
143 supplement 1Ba-i). In addition, compared with control mice, both the *COUP-TFI* and *-TFII*
144 genes were almost completely deleted in the hippocampal primordium at E14.5 in mutant
145 mice (Figure 1—figure supplement 1Bj-o). All the data above show that *RXCre* recombinase
146 could efficiently excise *COUP-TFI* and/or *COUP-TFII* in the early developing and adult
147 hippocampus.

148

149 **The *COUP-TFII* gene is required for the appropriate morphogenesis of the ventral**
150 **hippocampus but not of the dorsal hippocampus**

151 Given that the *COUP-TFII* gene is highly and specifically expressed in the adult ventral
152 hippocampus and the CH of the hippocampal primordium (Figure 1 and Figure 1—figure
153 supplement 1), we asked whether the *COUP-TFII* gene is required for the appropriate
154 morphogenesis of the hippocampus, particularly the ventral hippocampus. To answer this
155 question, we conducted Nissl staining with samples from the *COUP-TFII* single-gene
156 (*RXCre/+*; *COUP-TFII*$^{F/F}$ or *RXCre/+*; *CII*$^{F/F}$) knockout mouse model. In coronal sections,
157 compared with the control at 1M, the septal hippocampus was normal; unexpectedly, an
158 ectopic CA-like region was observed medially in the temporal hippocampus in the *COUP-*
159 *TFII* mutant, where there was the prospected posterior part of the medial amygdaloid nucleus

160 (MeP), indicated by the star (Figure 1Ba-f). The presence of the ectopic CA-like region in the
161 ventral but not dorsal hippocampus of the mutant was further confirmed at the prospected
162 MeP and prospected amygdalohippocampal area (AHi) in sagittal sections, as indicated by
163 the star (Figure 1Bg-l). Furthermore, immunofluorescence assays were performed to verify
164 whether specific lineages of the hippocampus were altered with sagittal sections, in which the
165 subregions of both the dorsal and ventral hippocampus were well displayed and distinguished.
166 Ctip2 is a marker for CA1 pyramidal neurons and DG granule neurons, and HuB is a marker
167 for CA3 pyramidal cells (Sugiyama, Osumi, & Katsuyama, 2014). The dorsal hippocampus
168 appeared normal in both the control and mutant mice at 1M (Figure 1Ca-l). Nonetheless,
169 compared with the observations in control mice, an ectopic HuB-positive CA3 pyramidal
170 neuron lineage, indicated by the star, and a duplicated Ctip2-positive CA1 pyramidal neuron
171 lineage, indicated by the arrowhead, were observed in the ventral hippocampal area in the
172 mutant (Figure 1Ca-f, m-r), revealing that there were ectopic CA1 and CA3 lineages in the
173 *COUP-TFII* mutants.
174 Consistent with the previous report (Leid et al., 2004), the expression of Ctip2 was detected
175 in the amygdala including the AHi and posteromedial cortical amygdaloid nucleus (PMCo);
176 in addition, Ctip2 was also highly expressed in the dorsal part of the MeP (MePD) in the
177 control (Figure 1Cb, n).
178 Intriguingly, compared with the controls at 1M, there were ectopic CA domains in the mutant
179 ventral hippocampus with the expense of the Ctip2 positive AHi and MePD amygdaloid
180 nuclei (Figure 1Ce, q), indicated by the arrows. Clearly, all the data above suggested that the
181 *COUP-TFII* gene is necessary to ensure the appropriate morphogenesis of the ventral
182 hippocampus.
183 At early embryonic stages, *COUP-TFII* was preferentially expressed in the CH (Figure 1—
184 figure supplement 1Ab,e), the organizer of the hippocampus, and at the adult stage, *COUP-*

TFII was also highly expressed in some amygdala nuclei such as the AHi and medial amygdaloid nucleus, which are adjacent to the ventral/temporal hippocampus (Figure 1Ae,h,n) (Tang et al., 2012). We would like to investigate the correlation of the CH and/or amygdala anlage with the duplicated ventral hippocampal domains in the *COUP-TFII* mutant in detail in our future study. The observations above suggest that *COUP-TFII* is not only specifically expressed in the ventral hippocampus but is also required for morphogenesis and probably the function of the ventral hippocampus. Since the ventral hippocampus participates in the regulation of emotion and stress, mutations in the *COUP-TFII* gene lead to CHDs, and the formation of the ventral hippocampus is disrupted in *COUP-TFII* adult mutant mice, we wondered whether CHD patients with *COUP-TFII* mutations also exhibit symptoms associated with psychiatric disorders such as depression, anxiety, or schizophrenia.

The *COUP-TFI* gene is required for the specification and differentiation of the dorsal CA1 identity

Next, we asked whether the deletion of the *COUP-TFI* gene by *RXCre* also affected the development of the hippocampus. Consistent with the previous finding in *Emx1Cre/+*; *COUP-TFI*$^{F/F}$ (*Emx1Cre/+*; *CI*$^{F/F}$) mutant mice (Flore et al., 2017), it was the septal/dorsal hippocampus, not the temporal/ventral hippocampus, that was specifically shrunken in both coronal (Figure 2Aa-f) and sagittal sections (Figure 2Ag-i) of *RXCre/+*; *COUP-TFI*$^{F/F}$ (*RXCre/+*; *CI*$^{F/F}$) mutant mice. Then, we asked whether the loss of the *COUP-TFI* gene caused abnormal specification and differentiation of hippocampal lineages. Compared with the control mice, *COUP-TFI* mutant mice had fewer HuB-positive CA3 pyramidal neurons, as indicated by the star; intriguingly, Ctip2-positive CA1 pyramidal neurons failed to be detected, as indicated by the arrowhead, with Ctip2-positive DG granule neurons unaltered in the dorsal hippocampus (Figure 2Ba-l). The loss of the dorsal CA1 pyramidal neuron identity

210 in mutant mice was further confirmed by Wfs1, another dorsal CA1 pyramidal neuron-
211 specific marker (Takeda et al., 2001) (Figure 2Ca-r). Nonetheless, the HuB-positive and
212 Ctip2-positive lineages were comparable in the ventral hippocampus between the control and
213 mutant mice (Figure 2Ba-f, m-r), even though the low expression of COUP-TFI was detected
214 there. Indeed, *COUP-TFI* is not only expressed at the highest level in the dorsal CA1 but is
215 also required for the specification and differentiation of dorsal CA1 pyramidal neurons,
216 among which place cells are essential for learning and memory (O'Keefe & Conway, 1978;
217 O'Keefe & Dostrovsky, 1971).

218 Given that dysplasia of the dorsal hippocampus was generated in both the *Emx1Cre* and
219 *RXCre* models (Flore et al., 2017) (Figure 2Aa-l), we asked whether the development of
220 dorsal CA1 pyramidal neurons was also abolished in *Emx1Cre/+*; *COUP-TFI*$^{F/F}$ mutant mice.
221 To answer this question, immunofluorescence staining was conducted first. Compared with
222 that in the control mice, the proportions of either the Wfs1- or Ctip2-positive CA1 domain
223 were reduced in the mutant mice at 3M (Figure 2—figure supplement 1Aa-h), indicating that
224 the differentiation of the dorsal CA1 pyramidal neurons was also compromised in the
225 *Emx1Cre* model, although it was less severe than that in the *RXCre* model. To make our
226 findings more consistent with previous studies, we further conducted experiments with the
227 *Emx1Cre* model. Afterward, to investigate the fine structure of the dorsal CA1 pyramidal
228 neurons, Golgi staining was performed. Compared with those of control mice, the numbers of
229 secondary dendrites and branch points of both the apical and basal dendrites were
230 significantly reduced in the dorsal CA1 pyramidal neurons of mutant mice at 3M (Figure 2—
231 figure supplement 1Ba-e). Then, the dorsal hippocampus-related spatial learning and memory
232 behavior test, the Morris water maze, was performed (Vorhees & Williams, 2006). Consistent
233 with a previous report (Flore et al., 2017), spatial learning and memory function was
234 significantly impaired in adult *Emx1Cre/+*; *COUP-TFI*$^{F/F}$ mice, compared with the control

235 mice (Figure 2—figure supplement 1C). The data above suggest that *COUP-TFI* is
236 imperative for the morphogenesis, lineage specification, and spatial learning and memory of
237 the dorsal hippocampus, and particularly, the compromised dorsal CA1 lineage could
238 contribute to the phenotypes associated with neurodevelopmental disorders, including ID or
239 ASD.
240

241 **The *COUP-TFI* and -*TFII* genes coordinate to ensure the genesis of the hippocampus**

242 Given that the loss of either *COUP-TFI* or -*TFII* leads to dysplasia of the dorsal or ventral
243 hippocampus, respectively, we asked whether these genes compensate for each other to
244 regulate the morphogenesis of the hippocampus. To answer this question, the *RXCre/+*;
245 *COUP-TFI*$^{F/F}$; *COUP-TFII*$^{F/F}$ (*RXCre/+*; *CI*$^{F/F}$; *CII*$^{F/F}$) double-mutant mouse was generated,
246 and a few homozygous double-gene mutant mice survived for approximately 3 weeks (3W).
247 Nonetheless, the reason for the lethality of the double-mutant mice is still unknown. Nissl
248 staining data showed that compared with that of control mice, the septal hippocampus was
249 severely shrunken, as indicated by the star, and the temporal hippocampus was barely
250 observed in the double-mutant mouse brains (Figure 3Aa-h). Unexpectedly, an ectopic
251 nucleus was observed in the region of the prospected temporal hippocampus, indicated by the
252 arrowhead, in the double-mutant mice (Figure 3Ag, h). In addition, compared with those of
253 controls, the regions with HuB-positive CA3 pyramidal neurons and Ctip2-positive or Prox1-
254 positive DG granule neurons were diminished in the double mutants; in particular, Ctip2-
255 positive dorsal CA1 pyramidal neurons could not be detected in the double mutants (Figure
256 3Ba-l). Furthermore, compared with the domains of controls, no HuB-positive, Ctip2-positive,
257 or Prox1-positive domains could be detected in the prospected temporal hippocampus in the
258 double mutants (Figure 3Ca-l). The results above suggest that the *COUP-TFI* and *COUP-*

259 *TFII* genes coordinate with each other to mediate the appropriate morphogenesis of the entire
260 hippocampus.
261
262 **_COUP-TF_ genes and adult neurogenesis in the hippocampus**
263 Given that the *COUP-TFI* or *-TFII* gene was highly expressed in the dorsal or ventral DG,
264 respectively (Figure 1A), and that RXCre recombinase could efficiently delete either gene in
265 the DG (Figure 1—figure supplement 1Ba-i), we asked whether the loss of the *COUP-TFI*
266 or/and *-TFII* gene in the DG would affect hippocampal adult neurogenesis. To answer this
267 question, the ventral DG, dorsal DG, and septal DG were chosen to perform
268 immunofluorescence assays in the *COUP-TFII* mutant, *COUP-TFI* mutant, and double
269 mutant models, respectively. Adult NSCs in the subgranular zone (SGZ) of the DG express
270 both GFAP and Nestin, and newborn granule neurons express Dcx (Gao, Arlotta, Macklis, &
271 Chen, 2007). The numbers of NSCs and newborn neurons in the SGZ of the DG were
272 comparable between control mice and either the *COUP-TFII* or *COUP-TFI* mutant mice
273 (Figure 3—figure supplement 1Aa-p, Ba-h); nonetheless, compared with those of control
274 mice, the numbers of the NSCs and newborn granule neurons in the SGZ of the DG were
275 reduced in the double mutants (Figure 3—figure supplement 1Aq-x, Bi-l), and the reduction
276 in both lineages was significant (Figure 3—figure supplement 1Ca, b). The data above
277 suggest that *COUP-TF* genes may coordinate with each other to execute essential functions
278 for appropriate hippocampal adult neurogenesis in the DG.
279
280 **Hippocampal trisynaptic connectivity was impaired in adult _COUP-TFII_ single-, _COUP-_**
281 **_TFI_ single-, and double-mutant mice**
282 Given that dysplasia of the hippocampus was observed in all three mouse models, we asked
283 whether the connectivity of the hippocampal trisynaptic circuit associated with the DG, CA3,

284 and CA1 regions (Amaral, 1993) was normal in these models. To answer this question, the
285 components of the trisynaptic circuit were characterized in the ventral hippocampus of
286 *COUP-TFII* mutants, the dorsal hippocampus of *COUP-TFI* mutants, and the septal
287 hippocampus of double mutants. Calretinin is a marker of mossy cells, Calbindin is a marker
288 of mossy fibers, and SMI312 is a marker of Schafer collaterals (Flore et al., 2017). Compared
289 with those of controls (Figure 4Aa, b, e, f, i, and j), the numbers of Calretinin-positive mossy
290 cells were reduced, Calbindin-positive mossy fibers were longer but thinner, and SMI312-
291 positive Schafer collaterals were thinner and discontinued in the ventral hippocampus of
292 *COUP-TFII* mutants at 1M (Figure 4Ac, d, g, h, k, and l). In addition, similar to the previous
293 report (Flore et al., 2017), the numbers of Calretinin-positive mossy cells were decreased,
294 Calbindin-positive mossy fibers were shorter and thinner, and SMI312-positive Schafer
295 collaterals were barely detected in the dorsal hippocampus of *COUP-TFI* mutants (Figure
296 4Ac, d, g, h, k, and l), compared with those of controls at 1M (Figure 4Ba, b, e, f, i, and j).
297 Moreover, compared with those of control mice (Figure 4Ca, b, e, f, i, and j), the numbers of
298 Calretinin-positive mossy cells were reduced; both Calbindin-positive mossy fibers and
299 SMI312-positive Schafer collaterals were barely detected in the prospected septal
300 hippocampus of the double mutants at 3W (Figure 4Cc, d, g, h, k, and l). Clearly, without
301 both *COUP-TF* genes, the connectivity of the hippocampal trisynaptic circuit was abolished
302 more severely. The observations above revealed that the formation of the trisynaptic circuit,
303 which is one of the fundamental characteristics of hippocampal neurophysiology (Basu &
304 Siegelbaum, 2015), was abnormal in all three mouse models, indicating that both the
305 morphology and functions of the hippocampus are most likely compromised in the loss of the
306 *COUP-TFI* and/or *COUP-TFII* gene.
307

The expression of several essential regulatory genes associated with early hippocampal development was abnormal in double mutants

Given that the hippocampus was almost completely diminished in double mutants, we asked how *COUP-TF* genes participated in the regulation of the early morphogenesis of the hippocampus. To answer this question, total RNA isolated from the whole telencephalons of control (n=5) and double-mutant-(n=3) embryos at E11.5 was used to generate cDNA, and then real-time quantitative PCR (RT–qPCR) assays were performed. As expected, compared with that of control mice, the expression of *COUP-TFI* and *COUP-TFII* was reduced significantly in the double mutant mice (Figure 5A). Then, we mainly focused on the intrinsic regulatory networks by analyzing the expression profiles of two groups of transcription factor genes. The *Foxg1*, *Gli3*, *Lhx2*, *Otx1, Otx2*, and *Pax6* genes, which are highly related to the early patterning of the dorsal telencephalon (Hebert & Fishell, 2008), were in the first group; *Axin2*, *Emx1*, *Emx2*, *Lef1*, *Lhx5*, and *Tcf4* genes, which are associated with early hippocampal development (Galceran et al., 2000; Moore & Iulianella, 2021; Tole et al., 2000; Yoshida et al., 1997; Zhao et al., 1999), were in the other group. The expression of the *Foxg1*, *Gli3*, *Lhx2*, *Otx1, Otx2*, and *Pax6* genes was comparable between the controls and double mutants (Figure 5A), indicating that the early patterning of the dorsal telencephalon is largely unaltered. Compared with that of control mice, the expression of the *Axin2*, *Emx2*, *Lef1*, and *Tcf4* genes was normal in the double mutants; interestingly, the expression of the *Emx1* and *Lhx5* transcripts was decreased significantly in the double mutants at E11.5 compared to that in control mice (Figure 5A). In addition, the reduced expression of Lhx5 protein was confirmed in the hippocampal primordium in the double mutants at E14.5 by immunofluorescence assay (Figure 5Ba-d, a'-d'). The expression of *Lhx2* was expanded ventrally into the choroid plexus in the *Lhx5* null mutant mice (Zhao et al., 1999), indicating that *Lhx5* could inhibit *Lhx2* expression locally. Interestingly, the expression of the Lhx2

protein was increased in the hippocampal primordium, indicated by the arrowhead, in the *COUP-TF* double-mutant mice at E14.5 (Figure 5Be-h, e'-h').

Next, we asked whether neural precursor cells (NPCs), intermediate progenitor cells (IPCs), or newborn neurons were affected in the early development of the hippocampus in double-mutant mice. Sox2 is a marker for NPCs, Tbr2 is a marker for IPCs, and NeuroD1 is a marker for newborn neurons (Yu, Marchetto, & Gage, 2014). The expression of Sox2 in the hippocampal regions was comparable between the control and double-mutant mice at E14.5 (Figure 5Ca-d, a'-d'), indicating that the generation of NPCs was normal. Nevertheless, compared with the control embryos, the numbers of Tbr2-positive IPCs and NeuroD1-positive newborn neurons were reduced in the double-mutant embryos (Figure 5Ce-l, 5Ce'-l'), and the reduction was significant (Figure 5D). Our observations were consistent with previous findings in *Lhx5* null mutant mice that the specification of the hippocampal NPCs was normal, but the later differentiation event was abolished (Zhao et al., 1999). All the data above suggest that *COUP-TF* genes may cooperate to ensure the early morphogenesis of the hippocampus by regulating the appropriate expression levels of *Lhx5* and *Lhx2* genes. Nevertheless, we could not exclude other possibilities that *COUP-TF* genes could also participate in the modulation of hippocampal development through *Emx1* or other genes.

Discussion

In our present study, we observed dorsal-high COUP-TFI and ventral-high COUP-TFII expression profiles in the adult hippocampus. The deletion of the *COUP-TFII* gene led to duplicated CA1 and CA3 domains of the ventral hippocampus. The loss of *COUP-TFI* resulted in the failed specification and differentiation of the dorsal CA1 pyramidal neuron lineage with a diminished dorsal hippocampus. Furthermore, the deficiency of both *COUP-TF* genes caused atrophy of almost the entire hippocampus, accompanied by compromised

358 generation of the CA1, CA3, and DG identities. In addition, the dorsal trisynaptic
359 components, ventral trisynaptic components, or entire trisynaptic components were abolished
360 in the corresponding *COUP-TFI* gene mutant, *COUP-TFII* gene mutant, or *COUP-TFI*/*-TFII*
361 double-gene mutant mice. Moreover, *COUP-TF* genes may cooperate to ensure the
362 appropriate morphogenesis and function of the hippocampus by regulating the *Lhx5-Lhx2*
363 axis.
364
365 **1. *COUP-TFII* governs the distinct characteristics of the ventral hippocampus**
366 Sixty years ago, the pioneering work of Milner and her colleagues discovered the essential
367 role of the hippocampus in declarative memory (Penfield & Milner, 1958; Scoville & Milner,
368 1957). Recently, accumulating evidence has supported the Moser theory that the
369 hippocampus is a heterogeneous structure with distinct characteristics of gene expression,
370 connectivity, and function along its dorsoventral axis (Bast, 2007; Fanselow & Dong, 2010;
371 Moser & Moser, 1998; Strange et al., 2014). The dorsal hippocampus marked in blue, in
372 which gene expression is similar to the neocortex, serves the "cold" cognitive function
373 associated with declarative memory and spatial navigation, and the ventral hippocampus
374 marked in red, in which gene expression is close to the hypothalamus and amygdala,
375 corresponds to the "hot" affective states related to emotion and anxiety (Figure 5—figure
376 supplement 1). The ventral hippocampus generates direct connectivity with the amygdala,
377 hypothalamus, medial prefrontal cortex (mPFC), and olfactory bulb (Cenquizca & Swanson,
378 2007; Hoover & Vertes, 2007; Kishi et al., 2000; Pitkanen et al., 2000; Roberts et al., 2007).
379 Nonetheless, thus far, the molecular and cellular mechanism of how the morphogenesis,
380 connectivity, and function of the ventral hippocampus is achieved has been largely unclear.
381 *COUP-TFII*, a nuclear receptor gene associated with heart disease (High et al., 2016), was
382 highly and exclusively expressed in the ventral hippocampus in adult mice and was expressed

383 ventrally in the CH of the hippocampal primordium in mouse embryos (Figure 1, Figure 1—
384 figure supplement 1, Figure 5Ea), indicating that the *COUP-TFII* gene may participate in the
385 regulation of the development and function of the ventral hippocampus. First, deficiency of
386 the *COUP-TFII* gene led to the duplication of the CA1 and CA3 domains of the ventral
387 hippocampus but not the dorsal hippocampus, which was confirmed both morphologically
388 and molecularly (Figure 1). Second, the formation of the trisynaptic circuit was specifically
389 abolished in the ventral hippocampus of *COUP-TFII* mutants (Figure 4), indicating that the
390 intrahippocampal circuit, information transfer, and function of the ventral hippocampus could
391 be compromised. Third, the ventral hippocampus generates neural circuits with the mPFC,
392 amygdala, nucleus accumbens, and hypothalamus, which are associated with
393 anxiety/behavioral inhibition, fear processing, pleasure/reward seeking, and the
394 neuroendocrine system, respectively (Anacker & Hen, 2017; Baik, 2020; Bryant & Barker,
395 2020; Cenquizca & Swanson, 2007; Herman et al., 2016; Kishi et al., 2000; O'Leary & Cryan,
396 2014; Pitkanen et al., 2000). These ventral hippocampal projections may be important for
397 processing information related to emotion and anxiety. Intriguingly, our previous studies
398 revealed that *COUP-TFII* is required for the development of the hypothalamus, amygdala,
399 and olfactory bulb (S. Feng et al., 2017; Tang et al., 2012; X. Zhou et al., 2015), all of which
400 generate functional neural circuits with the ventral hippocampus (Fanselow & Dong, 2010).
401 Particularly, both the hypothalamus and amygdala are also diminished in *RXCre/+*; *COUP-*
402 *TFII*$^{F/F}$ mutant mice (S. Feng et al., 2017; Tang et al., 2012), indicating that their
403 interconnectivities with the ventral hippocampus are abnormal. Thus, all the findings above
404 suggest that *COUP-TFII* is a novel and essential intrinsic regulator that controls the
405 morphogenesis, connectivity, and function of the ventral hippocampus.
406 Given that mutations of *COUP-TFII* are highly associated with CHDs and are required for
407 the distinct characteristics of the ventral hippocampus, we wondered whether CHD patients

408 carrying mutations of *COUP-TFII* also display symptoms of psychiatric disorders, such as
409 depression, anxiety, or schizophrenia, related to the ventral hippocampus. In our future study,
410 we would like to generate hippocampus-specific or hippocampal subdomain-specific
411 conditional knockout models to dissect distinct roles of the *COUP-TFII* gene in the
412 hippocampus, particularly in the ventral hippocampus, in detail.
413
414 **2. The *COUP-TFI* gene is required for the specification and differentiation of dorsal**
415 **CA1 pyramidal neurons**
416 The expression of *COUP-TFI*, another orphan nuclear receptor gene associated with
417 neurodevelopmental disorders (Bertacchi et al., 2020; Bosch et al., 2014; Contesse et al.,
418 2019), is high in the dorsal MP of the hippocampal primordium and is higher in the dorsal
419 hippocampus than in the ventral hippocampus (Figure 1, Figure 1—figure supplement 1,
420 Figure 5Ea) (Flore et al., 2017). Consistent with previous observations in *Emx1Cre/+*;
421 *COUP-TFI*$^{F/F}$ mutant mice (Flore et al., 2017), the dorsal hippocampus but not the ventral
422 hippocampus was specifically shrunken in *RXCre/+; COUP-TFI*$^{F/F}$ mice (Figure 2, Figure
423 5—figure supplement 1). *COUP-TFI* is expressed at the highest level in dorsal CA1
424 pyramidal neurons (Figure 1), indicating that the *COUP-TFI* gene may play a role in the
425 specification and differentiation of dorsal CA1 pyramidal neurons. As expected, the
426 expression of Ctip2 and Wfs1, two markers for dorsal CA1 pyramidal neurons, could not be
427 detected in the prospected dorsal CA1 domain in *RXCre/+*; *COUP-TFI*$^{F/F}$ mutant mice
428 (Figure 2); furthermore, *Emx1Cre/+*; *COUP-TFI*$^{F/F}$ mutant mice partially phenocopied the
429 compromised development of the dorsal CA1 lineage (Figure 2—figure supplement 1). It
430 seems that the spatiotemporal activity of RXCre recombinase is better or broader than that of
431 the Emx1Cre recombinase during the critical period of the specification of the dorsal CA1
432 pyramidal neuron identity. In addition, the Golgi staining assay revealed that the

433 development of the dendrites of the dorsal CA1 pyramidal neurons was abnormal (Figure 2—
434 figure supplement 1). All the observations above indicate that the *COUP-TFI* gene is not only
435 necessary for the morphogenesis of the dorsal hippocampus but is also required for the
436 specification and differentiation of the dorsal CA1 pyramidal neurons, among which there are
437 place cells. The identification of place cells fifty years ago was one of the most important
438 breakthroughs to understand the memory and hippocampus (O'Keefe & Dostrovsky, 1971).
439 Except for spatial information, place cells in the dorsal CA1 may also encode nonspatial
440 representations, such as time (Eichenbaum, 2017; Lisman et al., 2017). Notably, 95% of
441 patients carrying *COUP-TFI* mutations are associated with ID. Here, our observations
442 support the notion that the *COUP-TFI* gene is a novel intrinsic regulator that specifies the
443 dorsal CA1 pyramidal cell identity, which will benefit the understanding of both
444 neurophysiological functions of the hippocampus and the etiology of NDD including ID and
445 ASD.
446
447 **3. *COUP-TFI* and -*TFII* cooperate to ensure the appropriate morphogenesis of the**
448 **hippocampus by regulating the *Lhx5-Lhx2* axis in mice**
449 In wild-type mice, *COUP-TFI* and -*TFII* genes generated complementary expression profiles
450 in the embryonic hippocampal primordium with *COUP-TFI* in the dorsal MP, marked in
451 green; *COUP-TFII* in the ventral CH, marked in red (Figure 5Ea, Figure 1—figure
452 supplement 1); and in the adult hippocampus with high-COUP-TFI expression in the dorsal,
453 marked in green; and high-COUP-TFII expression in the ventral, marked in red (Figure 5Ea,
454 Figure 1). These findings indicated that *COUP-TF* genes may coordinate to regulate
455 hippocampal development. Indeed, as discussed above, the loss of either *COUP-TFI* or -*TFII*
456 only leads to dysplasia of the dorsal hippocampus (Flore et al., 2017) (Figure 2, Figure 2—
457 figure supplement 1) or ventral hippocampus (Figure 1), respectively; intriguingly, while

both genes are efficiently excised by *RXCre* in the hippocampal primordium (Figure 1—figure supplement 1), more severely shrunken hippocampi developed in the adult double knockout mice (Figure 3). The dosage-dependent severity of hippocampal abnormalities suggested that two nuclear receptor genes, *COUP-TFI* and *-TFII* could cooperate with each other to execute an imperative and intrinsic function in the development of the hippocampus.

It is known that both extrinsic signals and intrinsic factors participate in the regulation of the early development of the hippocampus. Notably, mutations of *Wnt3a* and *Lef1* eliminate the entire hippocampus (Galceran et al., 2000; S. M. Lee et al., 2000). Given that the expression of *Axin2*, *Lef1* and *Tcf4*, three Wnt-responsive transcription factor genes, was not altered in the *COUP-TF* double mutant (Figure 5A), it is unlikely that abnormal Wnt signaling is the cause of the compromised hippocampus. *Lhx5* is specifically expressed in the hippocampal primordium and is required for the morphogenesis of the hippocampus (Zhao et al., 1999). *Lhx2* is necessary for hippocampal development by repressing cortical hem fate (Mangale et al., 2008; Monuki et al., 2001). Agenesis of the hippocampus is observed in either *Lhx5* or *Lhx2* null mutant mice, and these genes particularly repress each other (Hebert & Fishell, 2008; Mangale et al., 2008; Roy et al., 2014; Zhao et al., 1999), indicating that the proper expression levels of *Lhx5* and *Lhx2* genes are imperative to maintain the appropriate development of the hippocampus (Figure 5Eb). The transcriptional expression of *Lhx5* but not *Lhx2* was reduced in *COUP-TF* double-mutant mice at E11.5, and three days later, decreased expression of the Lhx5 protein and enhanced expression of the Lhx2 protein were detected in the hippocampal primordium of double-mutant mice (Figure 5A-B). In addition, consistent with the observations in the *Lhx5* null mutant (Li et al., 2021; Miquelajáuregui et al., 2010), the generation of Sox2-positive hippocampal NPCs was not affected, but the development of Tbr2-positive IPCs and NeuroD1-positive newborn neurons was abnormal in *COUP-TF* double-mutant mice (Figure 5). Thus, our findings reveal a novel intrinsic

483 regulatory mechanism that *COUP-TFI* and *COUP-TFII*, two disease-associated nuclear
484 receptor genes, may cooperate with each other to ensure proper hippocampal morphogenesis
485 by regulating the *Lhx5-Lhx2* axis. Intriguingly, compared with the adult *Emx1Cre/+*; *COUP-*
486 *TFI*$^{F/F}$ mutant mice, the hippocampus was much smaller in the adult *Emx1Cre/+*; *COUP-*
487 *TFI*$^{F/F}$; *COUP-TFII*$^{F/F}$ double-gene mutant mice; nevertheless, both the dorsal and ventral
488 hippocampus were readily detected in double-gene mutants with *Emx1Cre* (our unpublished
489 observations). In addition, the discrepancy between the shrunken dorsal hippocampus
490 associated with the loss of *COUP-TFI* and the duplicated CA domains of the ventral
491 hippocampus associated with the deficiency of *COUP-TFII* suggested that the regulatory
492 network related to *COUP-TF* genes during the early morphogenesis of the hippocampus
493 could be much more complicated than suspected and should be investigated in our future
494 study.
495
496 **4. *COUP-TF* genes are imperative for the formation of the trisynaptic circuit**
497 The hippocampus and entorhinal cortex (EC) are interconnected through various neural
498 circuits to mediate the flow of the information associated with declarative memory (Basu &
499 Siegelbaum, 2015). Both direct and indirect glutamatergic circuits are involved in the relay of
500 information from the EC to the hippocampal CA1, and the trisynaptic pathway is the most
501 well-characterized indirect circuit. The EC sends sensory signals from association cortices
502 via the perforant path to the DG, then the DG granule cells send excitatory mossy fiber
503 projections to CA3 pyramidal neurons, and CA3 pyramidal neurons project to CA1 via the
504 Schaffer collaterals (H. Lee, GoodSmith, & Knierim, 2020). Consistent with the high
505 expression of COUP-TFI in the dorsal hippocampus and COUP-TFII in the ventral
506 hippocampus (Figure 1), the dorsal trisynaptic circuit is specifically damaged in *COUP-TFI*
507 mutants, as is the ventral trisynaptic circuit in *COUP-TFII* mutant mice. Moreover, the

508 hippocampal trisynaptic circuit was almost completely absent in the double mutants (Figure 4,
509 and our unpublished observations). The information transfer associated with the trisynaptic
510 circuits should be abolished particularly in the dorsal and/or the ventral hippocampus in the
511 above corresponding genetic mouse models. Interestingly, *COUP-TFI* is also required to
512 specify the medial EC cell fate (J. Feng et al., 2021). Therefore, the impaired formation and
513 function of trisynaptic circuits could be caused by the abnormal development of CA1, CA3,
514 DG or EC lineages. Nonetheless, given that newborn granule neurons are continuously
515 generated in the adult DG to integrate into the existing neural circuits essential for declarative
516 memory (Toda, Parylak, Linker, & Gage, 2019; Tuncdemir, Lacefield, & Hen, 2019) and that
517 hippocampal adult neurogenesis was severely compromised in the *COUP-TF* double mutant
518 (Figure 3—figure supplement 1), we could not exclude the possibility that impaired adult
519 neurogenesis may also contribute to the malformation and impaired function of the
520 trisynaptic pathway in double mutants.
521
522 The hippocampus is heterogeneous along its dorsoventral axis, and either the dorsal or
523 ventral hippocampus generates unique and distinguishable characteristics of gene expression
524 and connectivity, which enable the hippocampus to execute an integrative function from the
525 encoding and retrieval of certain declarative memory to adaptive behaviors. Lesions of the
526 dorsal hippocampus, which are essential for the cognitive process of learning and memory,
527 lead to amnesia and ID; while damage to the ventral hippocampus, which is imperative for
528 emotion and affection, is highly associated with psychiatric disorders including depression,
529 anxiety, and schizophrenia. Our findings in this study reveal novel intrinsic mechanisms by
530 which two nuclear receptor genes, *COUP-TFI* and *-TFII*, which are associated with NDD or
531 CHD, converge to govern the differentiation and integration of the hippocampus along the
532 dorsoventral axis morphologically and functionally. Furthermore, our present study provides

533 novel genetic model systems to investigate the crosstalk among the hippocampal complex in
534 gene expression, morphogenesis, cell fate specification and differentiation, connectivity,
535 functions of learning/memory and emotion/anxiety, adaptive behaviors, and the etiology of
536 neurological diseases. Nevertheless, many enigmas, such as whether and how the
537 abnormalities of either the dorsal or ventral hippocampus affect the characteristics of the
538 other, remain unsolved. In addition to the excitatory lineages and circuits, interneurons and
539 inhibitory circuits play vital roles in maintaining the plasticity and functions of the
540 hippocampus. We also wonder whether and how defects in interneurons and inhibitory
541 circuits could contribute to the compromised morphogenesis, connectivity, and functions of
542 the hippocampus and the etiology of psychiatric and neurological conditions including ID,
543 ASD, depression, anxiety, and schizophrenia.
544
545 **Materials and Methods**
546 **Animals**
547 *COUP-TFI-floxed* mice, *COUP-TFII-floxed* mice, *RXCre* mice and *Emx1Cre* mice used in
548 the study were of the C57B6/129 mixed background. The noon of vaginal plug day was set as
549 the embryonic day 0.5 (E0.5). All animal protocols were approved by the Animal Ethics
550 Committee of the Shanghai Institute of Biochemistry and Cell Biology. All methods were
551 performed in accordance with the relevant guidelines and regulations. Only the littermates
552 were used for the comparison.
553
554 **Nissl staining**
555 We used xylene to dewax paraffin sections, followed by rinsing with 100%, 95%, and 70%
556 ethanol. The slides were stained in 0.1% Cresyl Violet solution for 25 mins. Then the
557 sections were washed quickly in the water and differentiated in 95% ethanol. We used 100%

558 ethanol to dehydrate the slides, followed by rinsing with the xylene solution. Finally, the
559 neutral resin medium was used to mount the slides.
560
561 **Immunohistochemical (IHC) staining**
562 The paraffin sections were dewaxed and rehydrated as described above for Nissl staining.
563 The slides were boiled in 1×antigen retrieval solution (DAKO) under microwave conditions
564 for 15 min. After cooled to room temperature (RT), the slides were incubated with 3% H2O2
565 for 30 min. Then, the slides were treated with blocking buffer for 60 min at RT and then
566 incubated with the primary antibody in the hybridization buffer (10×diluted blocking buffer)
567 overnight (O/N) at 4 °C. The next day, the tyramide signal amplification kit (TSA)
568 (Invitrogen) was used according to the manufacturer's protocol. After being incubated with
569 1%TSA blocking buffer, the sections were treated with a biotinylated secondary antibody for
570 60 min at RT. After being washed with 1×PBS three times, the slides were incubated with
571 1×HRP-conjugated streptavidin for 1 h. Next, the tyramide working solution was prepared,
572 including the 0.15‰ H_2O_2 in distilled water, the 100×diluted tyramide substrate solution
573 (tyramide-488 or tyramide-594), and the amplification buffer. The sections were incubated
574 with the working solution for 10 min. Then the slides were counterstained with DAPI and
575 mounted with the antifade mounting medium (Southern Biotech) (S. Feng et al., 2017; Zhang
576 et al., 2020). Finally, the sections were observed and images were captured with a digital
577 fluorescence microscope (Zeiss).
578 The following primary antibodies were used in the study: mouse anti-COUP-TFI (1:1000,
579 R&D), mouse anti-COUP-TFII (1:2000, R&D), rabbit anti-HuB (1:500, Abcam), rat anti-
580 Ctip2 (1:500, Abcam), rabbit anti-Wfs1 (1:500, ProteinTech), goat anti-Prox1 (1:500, R&D),
581 rabbit anti-Calretinin (1:500, Sigma), rabbit anti-Calbindin (1:500, Swant), mouse anti-
582 SMI312(1:200, Covance), rabbit anti-Sox2 (1:500, Affinity BioReagents), rat anti-Tbr2

583 (1:500,Thermo Fisher), goat anti-NeuroD1 (1:200, Santa Cruz), goat anti-Lhx2 (1:200, Santa
584 Cruz), rabbit anti-Lhx5 (1:200, Millipore), mouse anti-GFAP(1:500, Sigma), rabbit anti-
585 Nestin (1:200, Santa Cruz), goat anti-Dcx (1:500, Santa Cruz). The following secondary
586 antibodies were used in the study: donkey anti-mouse IgG biotin-conjugated (1:400,
587 JacksonImmuno), donkey anti-rabbit IgG biotin-conjugated (1:400, JacksonImmuno), donkey
588 anti-goat IgG biotin-conjugated (1:400, JacksonImmuno), donkey anti-rat IgG biotin-
589 conjugated (1:400, JacksonImmuno).
590
591 **Western blotting**
592 We homogenized the isolated dorsal and ventral hippocampus tissues respectively in the
593 RIPA buffer (Applygen) with protease inhibitor cocktail (Sigma) and phosphatase inhibitors
594 (Invitrogen) and then centrifuged at the speed of 12,000 rpm for 30 mins. We collected the
595 supernatants and analyzed the total concentrations by the BCA kit (Applygen). Gradient
596 SDS-PAGE gels were used to separate the same amounts of protein sample (40 μg/lane), and
597 then the proteins were transferred to the PVDF membranes (Millipore). After being blocked
598 by the 3% BSA (Sigma) for 2h, the membranes that contained proteins were incubated by
599 primary antibodies at 4 °C O/N. The membranes were rinsed with 1×PBST three times for 10
600 mins and then treated with biotinylated secondary antibodies for 2h at RT. After washing
601 with 1×PBST, membranes were treated with the HRP-conjugated streptavidin for 1h at RT.
602 Finally, we used the chemiluminescence detection system (Tanon) to detect the bands. The
603 density of the protein band was analyzed by the software Image J.
604 The primary antibodies were used in the experiment as below: mouse anti-COUP-TFI
605 (1:2000, R&D), rabbit anti-COUP-TFII (1:3000, R&D). The following secondary antibodies
606 were applied in the study, including goat anti-mouse IgG biotin-conjugated (1:1000, KPL),
607 goat anti-rabbit IgG biotin-conjugated (1:1000, KPL).

608

609 **Golgi staining**

610 Deep anesthesia was performed before sacrificing the control and mutant mice, and the brains
611 were immediately isolated. The FD rapid GolgiStain kit (FD NeuroTech) was used to process
612 the brain tissue samples, which were immersed in an equal volume of immersion solution
613 mixed with solutions A and B and stored in the dark for two weeks at RT. At least 5ml of
614 immersion solution is used for each cubic meter of the tissue. For the best results, the
615 container of tissue was gently swirled from side to side twice a week during the incubating
616 period. And then the brain tissue was transferred to solution C in the dark at RT for at least
617 72 hours (up to 1 week). Finally, the tissues were cut into 100 μm thick slices with a cryostat
618 at -20°C to -22°C and transferred to gelatin-coated microscope slides containing solution C
619 using a sample retriever. The slices were dried naturally at RT. The concrete staining
620 procedure of the kit was followed using the manufactory's protocol. Then, the sections were
621 rinsed twice with double-distilled water for 4 minutes each time. The slices were placed in a
622 mixture of one volume of solution D, one volume of solution E, and two volumes of double
623 distilled water for 10 minutes and were rinsed twice with distilled water for 4 minutes each
624 time. Then the sections were dehydrated in 50%, 75%, and 95% ethanol for 4 minutes
625 respectively. Next, the slices were dehydrated in 100% ethanol 4 times for 4 minutes each
626 time. Finally, the sections were cleared in xylene and mounted with a neutral resin medium.

627

628 **Morris water maze**

629 By recording the time spent by the mice swimming in the water tank and finding the escape
630 platform hidden underwater, and the swimming trajectory, the Morris water maze test can
631 objectively reflect the spatial learning and memory ability of the mice. We poured tap water
632 into the water maze tank and added an appropriate amount of milky white food dye that was

633 mixed well. The height of the liquid level was about 1 cm higher than the escape platform,
634 and the water temperature was kept at about 25±1℃. At the same time, four markers of
635 different shapes were pasted on the four directions of the inner wall above the water tank to
636 distinguish different directions. The Morris water maze test was divided into the training
637 phase and the probe trial phase. The training phase lasted for 6 days, 4 times a day, and the
638 interval between each training was about 30 minutes. During training, the mice were placed
639 into the tank from the entry points of four different quadrants facing the inner wall, and their
640 latency was recorded from the time from entering the water to finding a hidden underwater
641 platform and standing on it. After the mouse found the platform, let it stay on the platform for
642 10 seconds before removing it. If the mouse failed to discover the platform 60 seconds after
643 entering the water, it was guided to find the platform and stayed for 10 seconds. Each mouse
644 was placed into the water tank from four water entry points and recorded as one training
645 session. The probe trial was carried out on the seventh day and the underwater platform was
646 removed. Each experimental mouse was put into the water tank at the same water entry point,
647 and allowed to move for 60 seconds. The time that each mouse spent in the quadrant, where
648 the platform was originally placed, was recorded.
649
650 **RNA isolation and quantitative real-time PCR**
651 Total RNAs were prepared from the whole telencephalon of the control (n=5) and double
652 mutant (n=3) mice at E11.5 respectively, with the TRIzol Reagent (Invitrogen) by following
653 the manufactory's protocol. Reverse-transcription PCR and real-time quantitative PCR assays
654 were performed as described previously (Tang et al., 2012). A student's t-test was used to
655 compare the means of the relative mRNA levels between the control group and mutant group.
656 Primer sequences are as follows:

Axin2-f, 5'-*ctgctggtcaggcaggag*-3', *Axin2-r*, 5'-*tgccagtttctttggctctt*-3'; *Coup-tfI-f*, 5'-*caaagccatcgtgctattca*-3', *Coup-tfI-r*, 5'-*cctgcaggctttcgatgt*-3'; *Coup-tfII-f*, 5'-*cctcaaagtgggcatgagac*-3', *Coup-tfII-r*, 5'-*tgggtaggctgggtaggag*-3'; *Emx1-f*, 5'-*ctctccgagacgcaggtg*-3', *Emx1-r,* 5'-*ctcagactccggcccttc*-3'; *Emx2-f*, 5'-*cacgcttttgagaagaacca*-3', *Emx2-r,* 5'-*gttctccggttctgaaacca*-3'; *Foxg1-f*, 5'-*gaaggcctccacagaacg*-3', *Foxg1-r*, 5'-*ggcaaggcatgtagcaaaag*-3'; *Gli3-f*, 5'-*tgatccatctcctattcctcca*-3', *Gli3-r*, 5'-*tctggatacgtcgggctact*-3'; *Lef1-f*, 5'-*tcctgaaatccccaccttct*-3', *Lef1-r*, 5'-*tgggataaacaggctgacct*-3'; *Lhx2-f*, 5'-*cagcttgcgcaaaagacc*-3', *Lhx2-r*, 5'-*taaaaggttgcgcctgaact*-3'; *Lhx5-f*, 5'-*tgtgcaataagcagctatcca*-3'; *Lhx5-r,* 5'-*caaactgcggtccgtaca*-3'; *Otx1-f*, 5'-*ccagagtccagagtccaggt*-3', *Otx1-r*, 5'-*ccgggttttcgttccatt*-3'; *Otx2-f*, 5'-*ggtatggacttgctgcatcc*-3', *Otx2-r*, 5'-*cgagctgtgccctagtaaatg*-3'; *Pax6-f*, 5'-*gttccctgtcctgtggactc*-3', *Pax6-r*, 5'-*accgcccttggttaaagtct*-3'; *Tcf4-f*, 5'-*aaatggccactgcttgatgt*-3', *Tcf4-r*, 5'-*gcaccaccggtactttgttc*-3'.

Quantification and statistical analysis

The number of specified immunofluorescent marker-positive cells was assessed by Image J Cell Counter in full image fields. Three brain sections per mouse were counted for each index. GraphPad Prism 7.0 (GraphPad) was used to perform statistical analysis. The data analysis used one-way analysis of variance (ANOVA), Dunnett's or Tukey's post hoc tests, and student's unpaired t-test. The data were expressed as the mean ± SEM. The data obtained from at least three independent replicates were used for statistical analysis. $P < 0.05$ was considered the significant statistical difference.

Acknowledgements

We thank Ms. Emerald Tang for her assistance with the manuscript. This work was supported by National Natural Science Foundation of China (31671508) and Guangdong Provincial Basic and Applied Basic Research Fund (2021A1515011299) to K.T; and in part by the National Key Basic Research and Development Program of China (2018YFA0108500,

2019YFA0801402, 2018YFA0800100, 2018YFA0108000, 2018YFA0107200, 2017YFA0102700), "Strategic Priority Research Program" of the Chinese Academy of Sciences, Grant No. (XDA16020501, XDA16020404) to N. J.

Author contributions

X.Y., W.R. designed and conducted the experiments. X.Y. and K.T. organized and wrote the manuscript. Z.W.L., S.F. and J.X.Y. assisted in conducting the experiments and analyzed the data. N.J. and K.T. conceived the project and approved the manuscript.

Competing interests

The authors declare no competing interests.

References

Amaral, D. G. (1993). Emerging principles of intrinsic hippocampal organization. *Current Opinion in Neurobiology, 3*(2), 225-229. doi:https://doi.org/10.1016/0959-4388(93)90214-J

Anacker, C., & Hen, R. (2017). Adult hippocampal neurogenesis and cognitive flexibility - linking memory and mood. *Nat Rev Neurosci, 18*(6), 335-346. doi:10.1038/nrn.2017.45

Armentano, M., Chou, S. J., Tomassy, G. S., Leingärtner, A., O'Leary, D. D., & Studer, M. (2007). COUP-TFI regulates the balance of cortical patterning between frontal/motor and sensory areas. *Nat Neurosci, 10*(10), 1277-1286. doi:10.1038/nn1958

Baik, J. H. (2020). Stress and the dopaminergic reward system. *Exp Mol Med, 52*(12), 1879-1890. doi:10.1038/s12276-020-00532-4

Bast, T. (2007). Toward an integrative perspective on hippocampal function: from the rapid encoding of experience to adaptive behavior. *Rev Neurosci, 18*(3-4), 253-281. doi:10.1515/revneuro.2007.18.3-4.253

Basu, J., & Siegelbaum, S. A. (2015). The Corticohippocampal Circuit, Synaptic Plasticity, and Memory. *Cold Spring Harb Perspect Biol, 7*(11). doi:10.1101/cshperspect.a021733

Bertacchi, M., Romano, A. L., Loubat, A., Tran Mau-Them, F., Willems, M., Faivre, L., . . . Studer, M. (2020). NR2F1 regulates regional progenitor dynamics in the mouse neocortex and cortical gyrification in BBSOAS patients. *Embo j, 39*(13), e104163. doi:10.15252/embj.2019104163

Bliss, T. V., & Lomo, T. (1973). Long-lasting potentiation of synaptic transmission in the dentate area of the anaesthetized rabbit following stimulation of the perforant path. *J Physiol, 232*(2), 331-356. doi:10.1113/jphysiol.1973.sp010273

Bosch, D. G., Boonstra, F. N., Gonzaga-Jauregui, C., Xu, M., de Ligt, J., Jhangiani, S., . . . Schaaf, C. P. (2014). NR2F1 mutations cause optic atrophy with intellectual disability. *Am J Hum Genet, 94*(2), 303-309. doi:10.1016/j.ajhg.2014.01.002

Bryant, K. G., & Barker, J. M. (2020). Arbitration of Approach-Avoidance Conflict by Ventral Hippocampus. *Front Neurosci, 14*, 615337. doi:10.3389/fnins.2020.615337

Cenquizca, L. A., & Swanson, L. W. (2007). Spatial organization of direct hippocampal field CA1 axonal projections to the rest of the cerebral cortex. *Brain Res Rev, 56*(1), 1-26. doi:10.1016/j.brainresrev.2007.05.002

Contesse, T., Ayrault, M., Mantegazza, M., Studer, M., & Deschaux, O. (2019). Hyperactive and anxiolytic-like behaviors result from loss of COUP-TFI/Nr2f1 in the mouse cortex. *Genes Brain Behav, 18*(7), e12556. doi:10.1111/gbb.12556

Eichenbaum, H. (2017). On the Integration of Space, Time, and Memory. *Neuron, 95*(5), 1007-1018. doi:10.1016/j.neuron.2017.06.036

Eichenbaum, H., & Cohen, N. J. (2014). Can we reconcile the declarative memory and spatial navigation views on hippocampal function? *Neuron, 83*(4), 764-770. doi:10.1016/j.neuron.2014.07.032

Fanselow, M. S., & Dong, H. W. (2010). Are the dorsal and ventral hippocampus functionally distinct structures? *Neuron, 65*(1), 7-19. doi:10.1016/j.neuron.2009.11.031

Feng, J., Hsu, W. H., Patterson, D., Tseng, C. S., Hsing, H. W., Zhuang, Z. H., . . . Chou, S. J. (2021). COUP-TFI specifies the medial entorhinal cortex identity and induces differential cell adhesion to determine the integrity of its boundary with neocortex. *Sci Adv, 7*(27). doi:10.1126/sciadv.abf6808

Feng, S., Xing, C., Shen, T., Qiao, Y., Wang, R., Chen, J., . . . Tang, K. (2017). Abnormal Paraventricular Nucleus of Hypothalamus and Growth Retardation Associated with Loss of Nuclear Receptor Gene COUP-TFII. *Sci Rep, 7*(1), 5282. doi:10.1038/s41598-017-05682-6

Flore, G., Di Ruberto, G., Parisot, J., Sannino, S., Russo, F., Illingworth, E. A., . . . De Leonibus, E. (2017). Gradient COUP-TFI Expression Is Required for Functional Organization of the Hippocampal Septo-Temporal Longitudinal Axis. *Cereb Cortex, 27*(2), 1629-1643. doi:10.1093/cercor/bhv336

Galceran, J., Miyashita-Lin, E. M., Devaney, E., Rubenstein, J. L., & Grosschedl, R. (2000). Hippocampus development and generation of dentate gyrus granule cells is regulated by LEF1. *Development, 127*(3), 469-482. doi:10.1242/dev.127.3.469

Gao, X., Arlotta, P., Macklis, J. D., & Chen, J. (2007). Conditional knock-out of beta-catenin in postnatal-born dentate gyrus granule neurons results in dendritic malformation. *J Neurosci, 27*(52), 14317-14325. doi:10.1523/jneurosci.3206-07.2007

Gould, E., & Cameron, H. A. (1996). Regulation of neuronal birth, migration and death in the rat dentate gyrus. *Dev Neurosci, 18*(1-2), 22-35. doi:10.1159/000111392

Hebert, J. M., & Fishell, G. (2008). The genetics of early telencephalon patterning: some assembly required. *Nat Rev Neurosci, 9*(9), 678-685. doi:10.1038/nrn2463

Herman, J. P., McKlveen, J. M., Ghosal, S., Kopp, B., Wulsin, A., Makinson, R., . . . Myers, B. (2016). Regulation of the Hypothalamic-Pituitary-Adrenocortical Stress Response. *Compr Physiol, 6*(2), 603-621. doi:10.1002/cphy.c150015

High, F. A., Bhayani, P., Wilson, J. M., Bult, C. J., Donahoe, P. K., & Longoni, M. (2016). De novo frameshift mutation in COUP-TFII (NR2F2) in human congenital diaphragmatic hernia. *Am J Med Genet A, 170*(9), 2457-2461. doi:10.1002/ajmg.a.37830

Hoover, W. B., & Vertes, R. P. (2007). Anatomical analysis of afferent projections to the medial prefrontal cortex in the rat. *Brain Struct Funct, 212*(2), 149-179. doi:10.1007/s00429-007-0150-4

Kandel, E. R., Dudai, Y., & Mayford, M. R. (2014). The molecular and systems biology of memory. *Cell, 157*(1), 163-186. doi:10.1016/j.cell.2014.03.001

Kim, B. J., Takamoto, N., Yan, J., Tsai, S. Y., & Tsai, M. J. (2009). Chicken Ovalbumin Upstream Promoter-Transcription Factor II (COUP-TFII) regulates growth and patterning of the postnatal mouse cerebellum. *Dev Biol, 326*(2), 378-391. doi:10.1016/j.ydbio.2008.11.001

Kishi, T., Tsumori, T., Ono, K., Yokota, S., Ishino, H., & Yasui, Y. (2000). Topographical organization of projections from the subiculum to the hypothalamus in the rat. *J Comp Neurol, 419*(2), 205-222. doi:10.1002/(sici)1096-9861(20000403)419:2<205::aid-cne5>3.0.co;2-0

Lee, H., GoodSmith, D., & Knierim, J. J. (2020). Parallel processing streams in the hippocampus. *Curr Opin Neurobiol, 64*, 127-134. doi:10.1016/j.conb.2020.03.004

Lee, S. M., Tole, S., Grove, E., & McMahon, A. P. (2000). A local Wnt-3a signal is required for development of the mammalian hippocampus. *Development, 127*(3), 457-467. doi:10.1242/dev.127.3.457

Leid, M., Ishmael, J. E., Avram, D., Shepherd, D., Fraulob, V., & Dolle, P. (2004). CTIP1 and CTIP2 are differentially expressed during mouse embryogenesis. *Gene Expr Patterns, 4*(6), 733-739. doi:10.1016/j.modgep.2004.03.009

Li, J., Sun, L., Peng, X. L., Yu, X. M., Qi, S. J., Lu, Z. J., . . . Shen, Q. (2021). Integrative genomic analysis of early neurogenesis reveals a temporal genetic program for differentiation and specification of preplate and Cajal-Retzius neurons. *PLoS Genet, 17*(3), e1009355. doi:10.1371/journal.pgen.1009355

Lisman, J., Buzsaki, G., Eichenbaum, H., Nadel, L., Ranganath, C., & Redish, A. D. (2017). Viewpoints: how the hippocampus contributes to memory, navigation and cognition. *Nat Neurosci, 20*(11), 1434-1447. doi:10.1038/nn.4661

Lodato, S., Tomassy, G. S., De Leonibus, E., Uzcategui, Y. G., Andolfi, G., Armentano, M., . . . Studer, M. (2011). Loss of COUP-TFI alters the balance between caudal ganglionic eminence- and medial ganglionic eminence-derived cortical interneurons and results in resistance to epilepsy. *J Neurosci, 31*(12), 4650-4662. doi:10.1523/jneurosci.6580-10.2011

Mangale, V. S., Hirokawa, K. E., Satyaki, P. R., Gokulchandran, N., Chikbire, S., Subramanian, L., . . . Monuki, E. S. (2008). Lhx2 selector activity specifies cortical identity and suppresses hippocampal organizer fate. *Science, 319*(5861), 304-309. doi:10.1126/science.1151695

Miquelajáuregui, A., Varela-Echavarría, A., Ceci, M. L., García-Moreno, F., Ricaño, I., Hoang, K., . . . Zhao, Y. (2010). LIM-homeobox gene Lhx5 is required for normal development of Cajal-Retzius cells. *J Neurosci, 30*(31), 10551-10562. doi:10.1523/jneurosci.5563-09.2010

Monuki, E. S., Porter, F. D., & Walsh, C. A. (2001). Patterning of the dorsal telencephalon and cerebral cortex by a roof plate-Lhx2 pathway. *Neuron, 32*(4), 591-604. doi:10.1016/s0896-6273(01)00504-9

Moore, S. A., & Iulianella, A. (2021). Development of the mammalian cortical hem and its derivatives: the choroid plexus, Cajal-Retzius cells and hippocampus. *Open Biol, 11*(5), 210042. doi:10.1098/rsob.210042

Moser, M. B., & Moser, E. I. (1998). Functional differentiation in the hippocampus. *Hippocampus, 8*(6), 608-619. doi:10.1002/(SICI)1098-1063(1998)8:6<608::AID-HIPO3>3.0.CO;2-7

O'Keefe, J., & Conway, D. H. (1978). Hippocampal place units in the freely moving rat: why they fire where they fire. *Exp Brain Res, 31*(4), 573-590. doi:10.1007/BF00239813

O'Keefe, J., & Dostrovsky, J. (1971). The hippocampus as a spatial map. Preliminary evidence from unit activity in the freely-moving rat. *Brain Res, 34*(1), 171-175. doi:10.1016/0006-8993(71)90358-1

O'Leary, O. F., & Cryan, J. F. (2014). A ventral view on antidepressant action: roles for adult hippocampal neurogenesis along the dorsoventral axis. *Trends Pharmacol Sci, 35*(12), 675-687. doi:10.1016/j.tips.2014.09.011

Penfield, W., & Milner, B. (1958). Memory deficit produced by bilateral lesions in the hippocampal zone. *AMA Arch Neurol Psychiatry, 79*(5), 475-497. doi:10.1001/archneurpsyc.1958.02340050003001

Pitkanen, A., Pikkarainen, M., Nurminen, N., & Ylinen, A. (2000). Reciprocal connections between the amygdala and the hippocampal formation, perirhinal cortex, and postrhinal cortex in rat. A review. *Ann N Y Acad Sci, 911*, 369-391. doi:10.1111/j.1749-6632.2000.tb06738.x

Roberts, A. C., Tomic, D. L., Parkinson, C. H., Roeling, T. A., Cutter, D. J., Robbins, T. W., & Everitt, B. J. (2007). Forebrain connectivity of the prefrontal cortex in the marmoset monkey (Callithrix jacchus): an anterograde and retrograde tract-tracing study. *J Comp Neurol, 502*(1), 86-112. doi:10.1002/cne.21300

Roy, A., Gonzalez-Gomez, M., Pierani, A., Meyer, G., & Tole, S. (2014). Lhx2 regulates the development of the forebrain hem system. *Cereb Cortex, 24*(5), 1361-1372. doi:10.1093/cercor/bhs421

Schuurmans, C., & Guillemot, F. (2002). Molecular mechanisms underlying cell fate specification in the developing telencephalon. *Curr Opin Neurobiol, 12*(1), 26-34. doi:10.1016/s0959-4388(02)00286-6

Scoville, W. B., & Milner, B. (1957). Loss of recent memory after bilateral hippocampal lesions. *J Neurol Neurosurg Psychiatry, 20*(1), 11-21. doi:10.1136/jnnp.20.1.11

Simeone, A., Gulisano, M., Acampora, D., Stornaiuolo, A., Rambaldi, M., & Boncinelli, E. (1992). Two vertebrate homeobox genes related to the Drosophila empty spiracles gene are expressed in the embryonic cerebral cortex. *EMBO J, 11*(7), 2541-2550. doi:10.1002/j.1460-2075.1992.tb05319.x

Strange, B. A., Witter, M. P., Lein, E. S., & Moser, E. I. (2014). Functional organization of the hippocampal longitudinal axis. *Nat Rev Neurosci, 15*(10), 655-669. doi:10.1038/nrn3785

Sugiyama, T., Osumi, N., & Katsuyama, Y. (2014). A novel cell migratory zone in the developing hippocampal formation. *J Comp Neurol, 522*(15), 3520-3538. doi:10.1002/cne.23621

Takeda, K., Inoue, H., Tanizawa, Y., Matsuzaki, Y., Oba, J., Watanabe, Y., . . . Oka, Y. (2001). WFS1 (Wolfram syndrome 1) gene product: predominant subcellular localization to endoplasmic reticulum in cultured cells and neuronal expression in rat brain. *Hum Mol Genet, 10*(5), 477-484. doi:10.1093/hmg/10.5.477

Tang, K., Rubenstein, J. L., Tsai, S. Y., & Tsai, M. J. (2012). COUP-TFII controls amygdala patterning by regulating neuropilin expression. *Development, 139*(9), 1630-1639. doi:10.1242/dev.075564

Toda, T., Parylak, S. L., Linker, S. B., & Gage, F. H. (2019). The role of adult hippocampal neurogenesis in brain health and disease. *Mol Psychiatry, 24*(1), 67-87. doi:10.1038/s41380-018-0036-2

Tole, S., Goudreau, G., Assimacopoulos, S., & Grove, E. A. (2000). Emx2 is required for growth of the hippocampus but not for hippocampal field specification. *J Neurosci, 20*(7), 2618-2625. Retrieved from https://www.ncbi.nlm.nih.gov/pubmed/10729342

Tuncdemir, S. N., Lacefield, C. O., & Hen, R. (2019). Contributions of adult neurogenesis to dentate gyrus network activity and computations. *Behav Brain Res, 374*, 112112. doi:10.1016/j.bbr.2019.112112

Tyng, C. M., Amin, H. U., Saad, M. N. M., & Malik, A. S. (2017). The Influences of Emotion on Learning and Memory. *Front Psychol, 8*, 1454. doi:10.3389/fpsyg.2017.01454

Vorhees, C. V., & Williams, M. T. (2006). Morris water maze: procedures for assessing spatial and related forms of learning and memory. *Nat Protoc, 1*(2), 848-858. doi:10.1038/nprot.2006.116

Yang, X., Feng, S., & Tang, K. (2017). COUP-TF Genes, Human Diseases, and the Development of the Central Nervous System in Murine Models. *Curr Top Dev Biol, 125*, 275-301. doi:10.1016/bs.ctdb.2016.12.002

Yoshida, M., Suda, Y., Matsuo, I., Miyamoto, N., Takeda, N., Kuratani, S., & Aizawa, S. (1997). Emx1 and Emx2 functions in development of dorsal telencephalon. *Development, 124*(1), 101-111. doi:10.1242/dev.124.1.101

Yu, D. X., Marchetto, M. C., & Gage, F. H. (2014). How to make a hippocampal dentate gyrus granule neuron. *Development, 141*(12), 2366-2375. doi:10.1242/dev.096776

Zhang, K., Yu, F., Zhu, J., Han, S., Chen, J., Wu, X., . . . Tang, K. (2020). Imbalance of Excitatory/Inhibitory Neuron Differentiation in Neurodevelopmental Disorders with an NR2F1 Point Mutation. *Cell Rep, 31*(3), 107521. doi:10.1016/j.celrep.2020.03.085

Zhao, Y., Sheng, H. Z., Amini, R., Grinberg, A., Lee, E., Huang, S., . . . Westphal, H. (1999). Control of hippocampal morphogenesis and neuronal differentiation by the LIM homeobox gene Lhx5. *Science, 284*(5417), 1155-1158. doi:10.1126/science.284.5417.1155

Zhou, C., Qiu, Y., Pereira, F. A., Crair, M. C., Tsai, S. Y., & Tsai, M. J. (1999). The nuclear orphan receptor COUP-TFI is required for differentiation of subplate neurons and guidance of thalamocortical axons. *Neuron, 24*(4), 847-859. doi:10.1016/s0896-6273(00)81032-6

Zhou, C., Tsai, S. Y., & Tsai, M. J. (2001). COUP-TFI: an intrinsic factor for early regionalization of the neocortex. *Genes Dev, 15*(16), 2054-2059. doi:10.1101/gad.913601

Zhou, X., Liu, F., Tian, M., Xu, Z., Liang, Q., Wang, C., . . . Yang, Z. (2015). Transcription factors COUP-TFI and COUP-TFII are required for the production of granule cells in the mouse olfactory bulb. *Development, 142*(9), 1593-1605. doi:10.1242/dev.115279

905 **Figure legends**

906

907 **Figure 1. Duplicated CA1 and CA3 domains are generated in the ventral hippocampus**

908 **of *RXCre/+*; *CII$^{F/F}$* mutant mice.**

909 **A,** The expression of COUP-TFI (**a, d, g, j, m**) and COUP-TFII (**b, e, h, k, n**) in coronal

910 sections (**a-f**) and sagittal sections (**g-o**) of the hippocampus at postnatal month 1 (1M);

911 representative Western blots and quantitative densitometry data for the expression of COUP-

912 TFI and COUP-TFII in the dorsal and ventral hippocampus at 1M (**p-q**). **B,** In coronal

913 sections along the rostrocaudal axis (**a-f**) and sagittal sections along the lateral-medial axis

914 (**g-l**) of the hippocampus in mutant mice, compared with that in control mice (**a-c**, **g-i**), the

915 ectopic CA-like structure, indicated by the star, was observed in the ventral region in *COUP-*

916 *TFII* gene mutant (*RXCre/+*; *CII$^{F/F}$)* mice at 1M (**d-f**, **j-l**). **C,** The expression of HuB and

917 Ctip2 in the corresponding inserted area in **a-f** under a high magnification objective lens at

918 1M (**g-r**); compared with those of control mice (**a-c**, **g-i**, **m-o**), the duplicated HuB-positive

919 CA3 domain, indicated by the star, and Ctip2-positive domains, indicated by the arrowhead,

920 were specifically observed in the ventral hippocampus (**d-f, p-r**) but not in the dorsal

921 hippocampus (**d-f**, **j-l**) of *COUP-TFII* mutant mice at 1M; Ctip2 positive AHi and MePD

922 amygdaloid nuclei were barely observed in the *COUP-TFII* mutant mice, indicated by the

923 arrows, instead of the ectopic CA domains at the prospected amygdaloid regions (**e-f**, **q-r**).

924 Data are expressed as the mean ± SEM. *Student's t test*, $^{*}P<0.05$, $^{**}P<0.01$. dCA1, dorsal

925 CA1; dCA3, dorsal CA3; dDG, dorsal dentate gyrus; vCA1, ventral CA1; vCA3, ventral CA3;

926 vDG, ventral dentate gyrus; PMCo, posteromedial cortical amygdaloid nucleus; AHi,

927 amygdalohippocampal area; dHPC, dorsal hippocampus; vHPC, ventral hippocampus; AMY,

928 amygdala nuclei; CTX, cortex; MePD, posterodorsal part of the medial amygdaloid nucleus.

929 Scale bars, **Aa-c**, **Ad-f**, **Aj-o**, **Cg-r**, 100 μm; **Ag-i**, **Ba-l, Ca-f**, 200μm.

930

931 **Figure 1—figure supplement 1. The expression of *COUP-TF* genes in the early**
932 **developing hippocampus and different conditional knock mouse models.**
933 **A,** The expression of *COUP-TFI* and *COUP-TFII* genes in the developing hippocampus at
934 E12.5 (**a-c**), E14.5 (**d-f**), and P0 (**g-l**). **B,** Compared with that of control mice (**a-c**), *COUP-*
935 *TFII* is efficiently deleted by RXCre recombinase in the hippocampus of *COUP-TFII* mutant
936 mice at 1M (**d-f**); *COUP-TFI* is clearly deleted by RXCre recombinase in the hippocampus
937 of *COUP-TFI* mutant mice at 1M (**g-i**). Compared with that of control mice (**j-l**), COUP-TFI
938 and COUP-TFII were efficiently deleted by RXCre recombinase at the hippocampal
939 primordium, including MP and CH, in *COUP-TFI/-TFII* double-mutant mice at E14.5 (**m-o**).
940 MP, medial pallium; CH, cortical hem; HPC, hippocampus; dHPC, dorsal hippocampus;
941 vHPC, ventral hippocampus. Scale bars, **Aa-f**, **Bj-o**, 200 μm; **Ag-l**, **Ba-i**, 100 μm.
942
943 **Figure 2. The specification and differentiation of the dorsal CA1 lineage failed with the**
944 **dysplastic dorsal hippocampus in *RXCre/+*; *CI$^{F/F}$* mutant mice.**
945 **A,** In coronal sections along the rostrocaudal axis (**a-f**) and sagittal sections along the lateral-
946 medial axis (**g-l**) of the hippocampus, compared with that of control mice (**a-c**, **g-i**), the dorsal
947 hippocampus was shrunken, indicated by the star, in *COUP-TFI* gene mutant (*RXCre/+;CI$^{F/F}$*)
948 mice at 1M (**d-f**, **j-l**). **B,** The expression of HuB and Ctip2 in the corresponding inserted area
949 in **a-f** under a high magnification objective lens at 1M (**g-r**); compared with that of control
950 mice (**a-c**, **g-i**, **m-o**), the HuB-positive CA3 domain was reduced in the dorsal hippocampus,
951 especially the Ctip2-positive dorsal CA1, which was barely detected in *COUP-TFI* mutant
952 mice at 1M (**d-f**, **j-l**), while their expression in the ventral hippocampus was comparable
953 between the controls and mutants (**d-f**, **p-r**). **C,** The expression of HuB and Wfs1 in the
954 corresponding inserted area in **a-f** under a high magnification objective lens at 1M (**g-r**); the
955 expression of HuB and the dCA1 marker Wfs1 in the control (**a-c**, **g-i**, **m-o**) and *COUP-TFII*

956 mutant mice (**d-f**, **j-l**, **p-r**) at 1M. Wfs1-positive dorsal CA1 could not be detected in *COUP-*
957 *TFI* mutant mice at 1M, as indicated by the arrowhead. HPC, hippocampus; dHPC, dorsal
958 hippocampus; vHPC, ventral hippocampus. Scale bars, **Aa-l**, **Ba-f**, **Ca-f,** 200 μm; **Bg-r**, **Cg-r,**
959 100 μm.
960
961 **Figure 2—figure supplement 1. Defects in *Emx1Cre/+*; *COUP-TFI*$^{F/F}$ mutant mice.**
962 **A,** Immunofluorescence staining data showed that compared with those of control mice (**a, c,**
963 **e, g**), the proportions of either the Wfs1- or Ctip2-positive dorsal CA1 domain were reduced
964 in *Emx1Cre/+*; *COUP-TFI*$^{F/F}$ mutant mice at 3M (**b, d, f, h**). **B,** Golgi staining showed that
965 compared with those of controls, the numbers of branch points and secondary dendrites of
966 both apical and basal dendrites were significantly reduced in the dorsal hippocampal CA1
967 pyramidal neurons of *Emx1Cre/+*; *COUP-TFI*$^{F/F}$ mutant mice (**a-c**). **C,** The Morris water
968 maze behavior test showed that compared with that of controls, spatial learning and memory
969 were significantly damaged in *Emx1Cre/+*; *COUP-TFI*$^{F/F}$ mutant mice. Data are expressed as
970 the mean ± SEM. *Student's t test*, $^{*}P<0.05$, $^{**}P<0.01$, $^{***}P<0.001$. Scale bars, **Aa-h,** 100 μm;
971 **Ba-b,** 50 μm.
972
973 **Figure 3. Defects in the hippocampus in *RXCre/+*; *CI*$^{F/F}$; *CII*$^{F/F}$ double-gene mutant**
974 **mice.**
975 **A,** In coronal sections along the rostrocaudal axis, compared with control mice (**a-d**), the
976 hippocampus was atrophic in *RXCre/+*; *CI*$^{F/F}$*; CII*$^{F/F}$ double mutant mice, indicated by the
977 star, and an ectopic unknown nucleus was observed in the caudal plates, indicated by the
978 arrowhead (**e-h**). **B,** Compared with that of control mice (**a-c**, **g-i**), the expression of HuB,
979 Ctip2, and Prox1 was decreased in the hippocampus of *COUP-TFI/-TFII* double-gene mutant
980 mice at 3 weeks postnatal (3W) (**d-f**, **j-l**). **C,** Compared with that of control mice (**a-c**, **g-i**),

981 the expression of HuB could not be detected in the presumptive CA3 domain, and the
982 expression of Ctip2 or Prox1 could not be detected in the presumptive DG domain of the
983 prospected ventral hippocampus of *RXCre/+*; $CI^{F/F}$; $CII^{F/F}$ double mutant mice. Scale bars,
984 **Aa-h**, 200 μm; **Ba-l**, **Ca-l,** 100 μm.
985
986 **Figure 3—figure supplement 1. Adult neurogenesis was abnormal in the hippocampi of**
987 ***COUP-TFI/-TFII* double-gene mutant mice.**
988 **A,** The expression of GFAP and Nestin, markers of NSCs, in the SGZ of the vDG in control
989 and *COUP-TFII* mutant mice at 1M (**a-h**), in the SGZ of the dDG in control and *COUP-TFI*
990 mutant mice at 1M (**i-p**) and in the SGZ of the DG in control and *COUP-TFI/-TFII* double-
991 gene mutant mice at 3W (**q-x**). **B**, The expression of Dcx, a marker of newborn neurons, in
992 the SGZ of the vDG in control and *COUP-TFII* mutant mice at 1M (**a-d**), in the SGZ of the
993 dDG in control and *COUP-TFI* mutant mice at 1M (**e-h**) and in the SGZ of the DG in control
994 and *COUP-TFI/-TFII* double-gene mutant mice at 3W (**i-l**). **C,** Quantitative analysis of
995 GFAP/Nestin-positive cells (**a**) and Dcx-positive cells (**b**) in the SGZ of the DG in control
996 and *COUP-TFI/-TFII* double-gene mutant mice at 3W. The numbers of GFAP and Nestin
997 double-positive NSCs and Dcx-positive newborn neurons were significantly reduced in
998 double-mutant mice. Data are expressed as the mean ± SEM. *Student's t test*, $^{**}P<0.01$,
999 $^{***}P<0.001$. vDG, ventral DG; dDG, dorsal DG; NSC, neural stem cell; SGZ, subgranular
1000 zone. Scale bars, **Aa-x**, 50 μm; **Ba-l**, 100 μm.
1001
1002 **Figure 4. The impairment of hippocampal trisynaptic connectivity in *COUP-TFII***
1003 **single-gene, *COUP-TFI* single-gene, and *COUP-TFI/-TFII* double-gene mutant mice.**
1004 **A,** The expression of Calretinin, Calbindin, and SMI312 in the ventral hippocampus of the
1005 control (**a-b**, **e-f**, **i-j**) and *COUP-TFII* single-gene mutant mice (**c-d**, **g-h**, **k-l**). **B,** The

1006 expression of Calretinin, Calbindin, and SMI312 in the dorsal hippocampus of the control (**a-**
1007 **b**, **e-f**, **i-j**) and *COUP-TFI* single-gene mutant mice (**c-d**, **g-h**, **k-l**). **C,** The expression of
1008 Calretinin, Calbindin, and SMI312 in the hippocampus of the control (**a-b**, **e-f**, **i-j**) and
1009 *COUP-TFI*/*-TFII* double-gene mutant mice (**c-d**, **g-h**, **k-l**). vHPC, ventral hippocampus;
1010 dHPC, dorsal hippocampus; HPC, hippocampus. Scale bars, **Aa-l**, **Ba-l**, **Ca-l**, 100 μm.
1011
1012 **Figure 5. *COUP-TF* genes regulate the expression of key genes associated with early**
1013 **hippocampal development.**
1014 **A,** The expression profiles of genes involved in hippocampal development in control and the
1015 double mutant mice at E11.5. **B,** Compared with that of control mice (**a-b**, **a'-b'**), the
1016 expression of Lhx5 was reduced in double-mutant mice at E14.5 (**c-d**, **c'-d'**); compared with
1017 that of control mice (**e-f**, **e'-f'**), the expression of Lhx2 was increased in double-mutant mice
1018 at E14.5 (**g-h**, **g'-f'**). **C,** Compared with that of control mice (**a-b**, **a'-b'**), the expression of
1019 Sox2 was normal in double-mutant mice at E14.5 (**c-d**, **c'-d'**); compared with that of control
1020 mice (**e-f**, **e'-f'**), the expression of Tbr2 was decreased in *COUP-TF* mutant mice at E14.5 (**g-**
1021 **h**, **g'-h'**); compared with that of control mice (**i-j**, **i'-j'**), the expression of NeuroD1 was
1022 reduced in double-mutant mice at E14.5 (**k-l**, **k'-l'**). **D,** Quantitative analysis of Tbr2-positive
1023 cells and NeuroD1-positive cells in **Ce'-h'** and **Ci'-l'**. **E,** In the hippocampal primordium of
1024 the early embryo, *COUP-TFI* is expressed dorsally in the MP, and *COUP-TFII* is expressed
1025 ventrally in the CH. In the mature adult hippocampus, the expression of *COUP-TFI* is higher
1026 in the dorsal hippocampus, which is related to spatial learning and memory, and the
1027 expression of *COUP-TFII* is mainly in the ventral hippocampus, which is associated with
1028 emotion and anxiety (**a**). Our findings support a novel molecular mechanism by which
1029 *COUP-TFI* and *COUP-TFII* may cooperate to ensure the appropriate morphogenesis and
1030 functions of the hippocampus by modulating the *Lhx5-Lhx2* axis (**b**). Data are expressed as

1031 the mean ± SEM. *Student's t test*, $^{**}P<0.01$. HP, hippocampal primordium; DP, dorsal
1032 pallium; MP, medial pallium; CH, cortical hem; ChP, choroid plexus. Scale bars, **Ba-d**, **Be-h**,
1033 **Ca-d**, **Ce-h**, **Ci-l**, 200 μm; **Ba'-d'**, **Be'-h'**, **Ce'-h'**, **Ci'-l'**, 50 μm.

1034

1035 **Figure 5—figure supplement 1. *COUP-TFI* and *-TFII* genes coordinate to control**
1036 **distinct characteristics of the hippocampus.**

1037 Roles of *COUP-TFI* and *COUP-TFII* genes in the development and function of the
1038 hippocampus and the association with neurological diseases. *COUP-TFI* is required for the
1039 morphogenesis of the dorsal hippocampus and the specification of dorsal CA1 pyramidal
1040 neuron lineage, which are associated with neurodevelopmental disorders, including ID and
1041 ASDs. *COUP-TFII* is required to prevent the duplication of the CA1 and CA3 lineages of the
1042 ventral hippocampus, which may be related to psychiatric diseases such as depression,
1043 anxiety, or schizophrenia. The *COUP-TFI* and *COUP-TFII* genes are novel intrinsic
1044 regulatory genes, which cooperate with each other to ensure the early morphogenesis of the
1045 hippocampus.

1046

Figure 1, Yang et al.

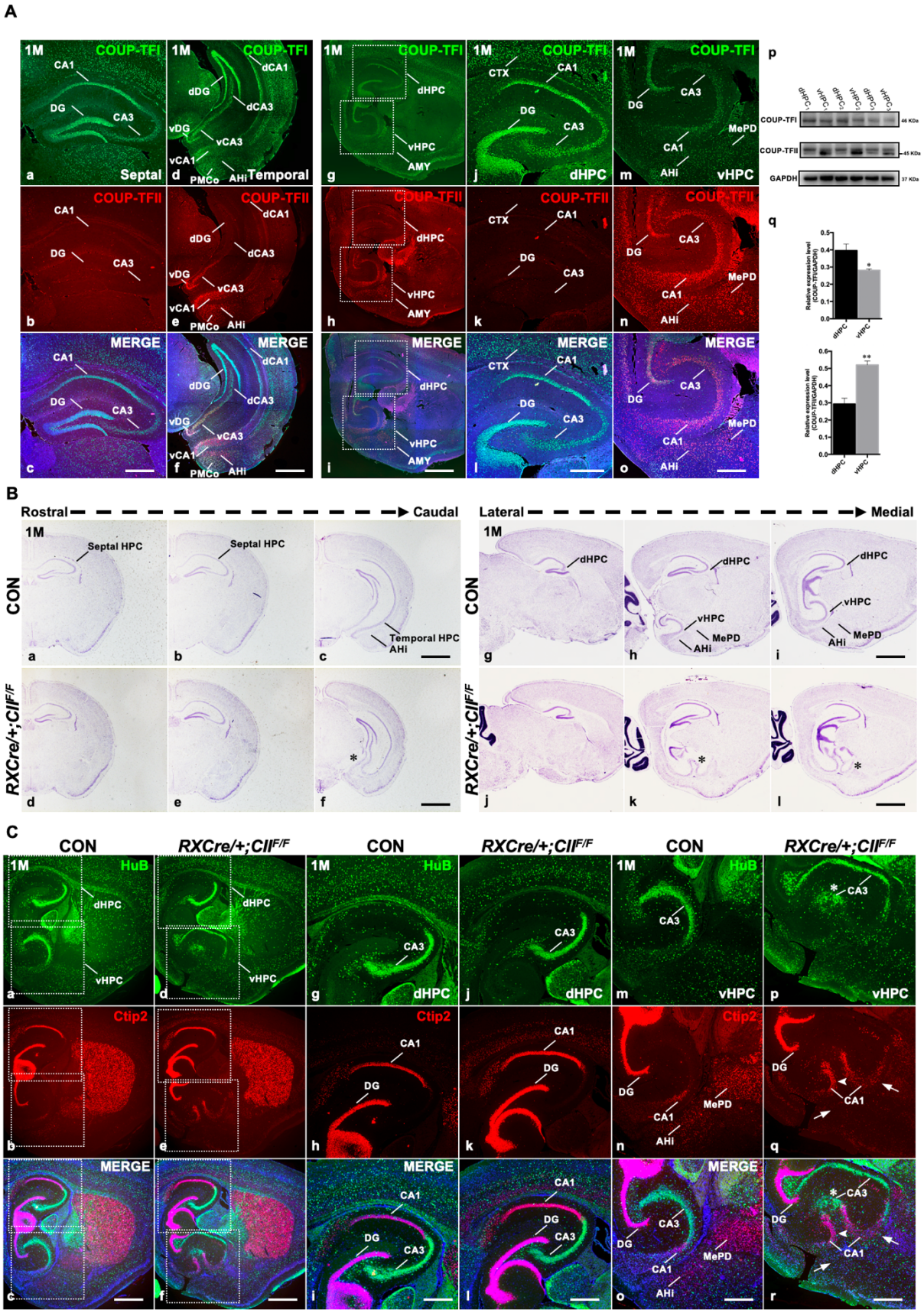

Figure 1—figure supplement 1, Yang et al.

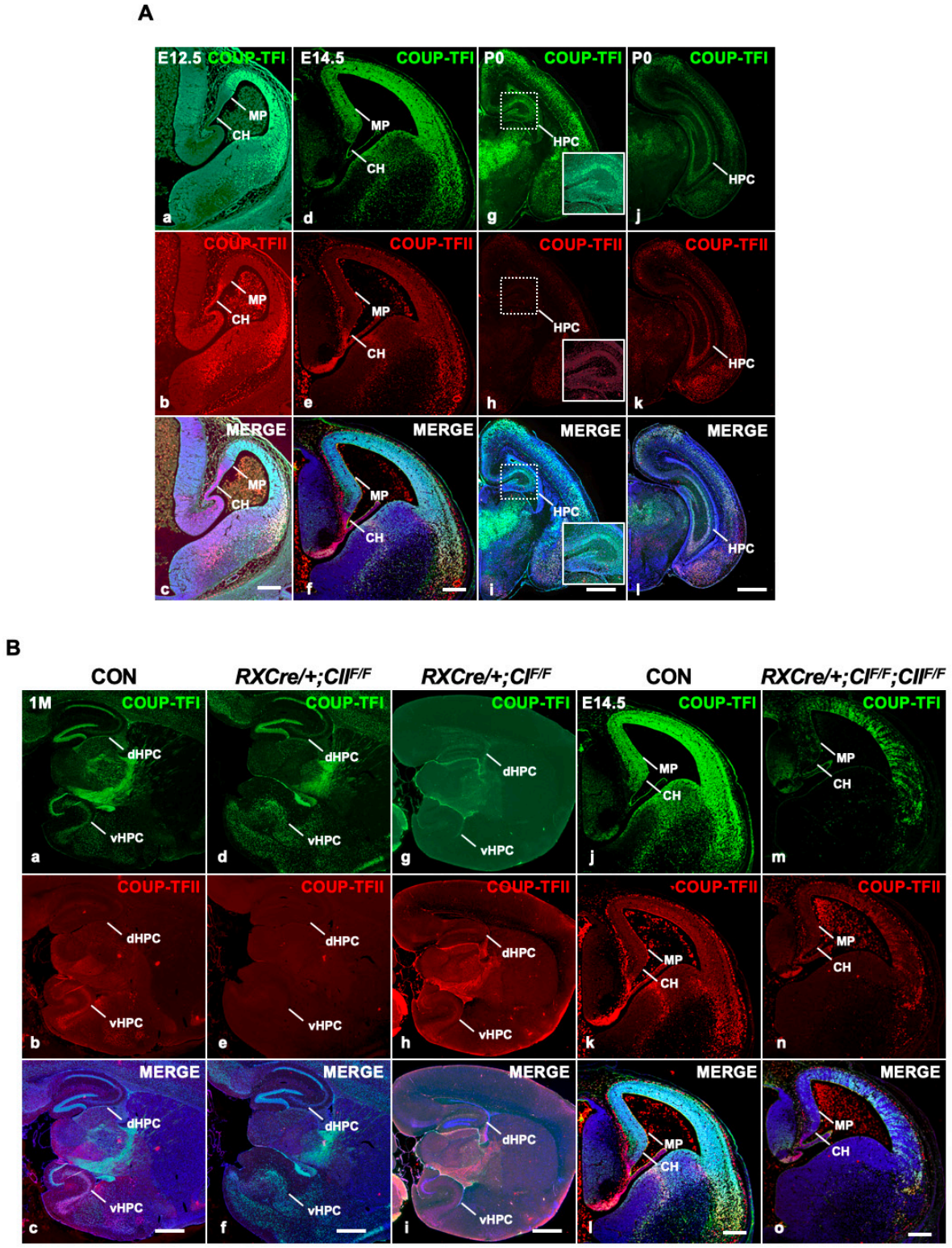

Figure 2, Yang et al.

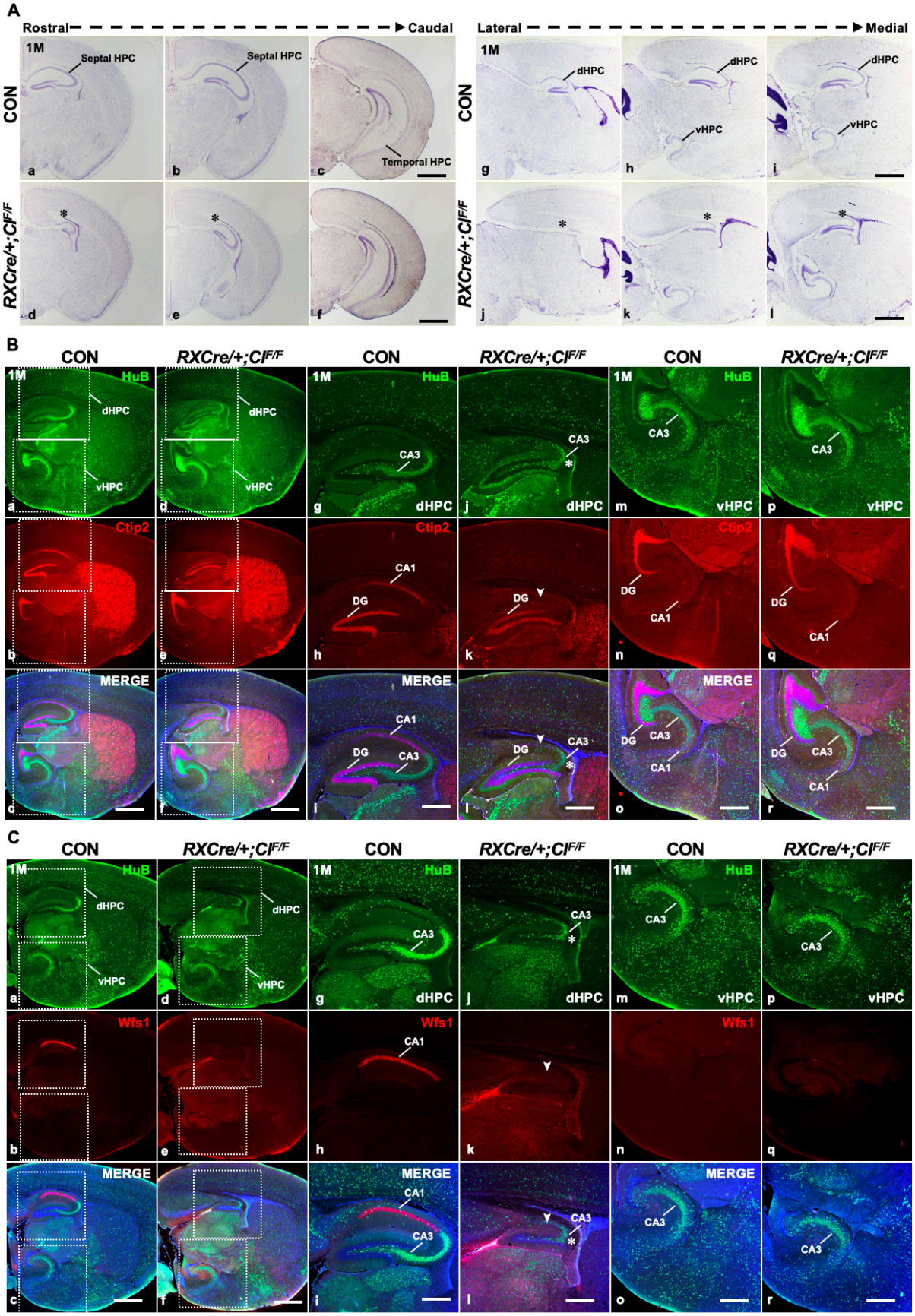

Figure 2—figure supplement 1, Yang et al.

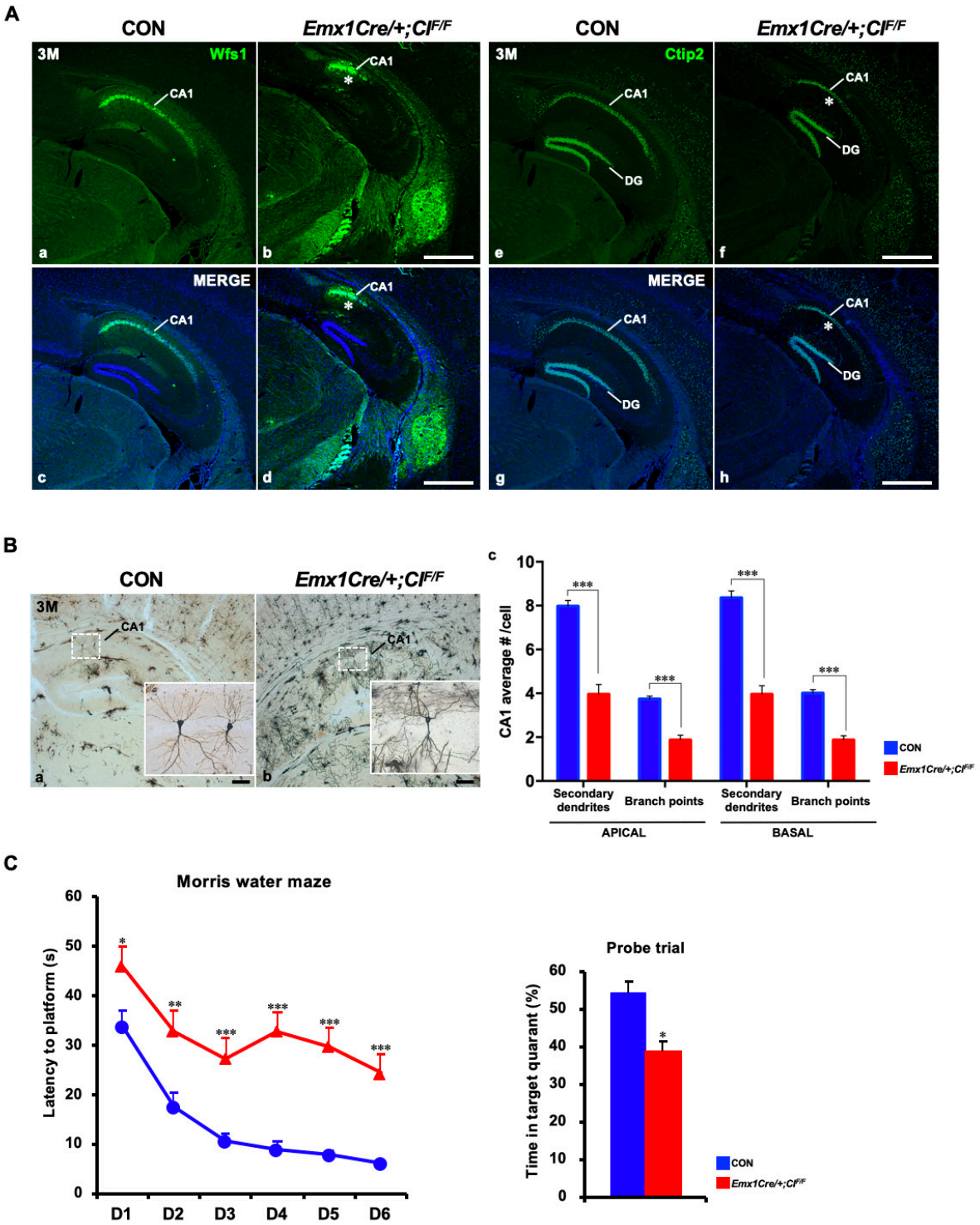

Figure 3, Yang et al.

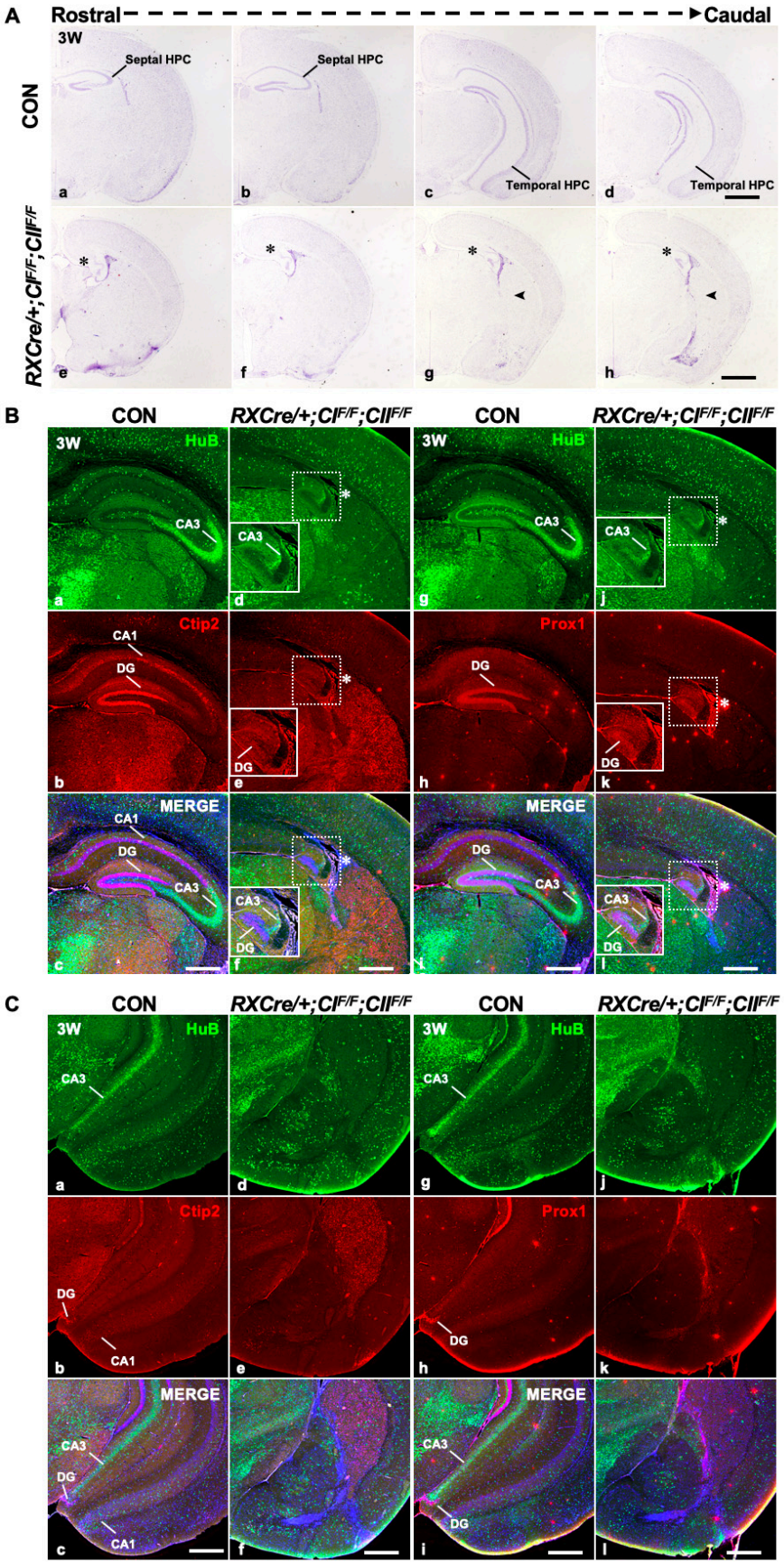

Figure 3—figure supplement 1, Yang et al.

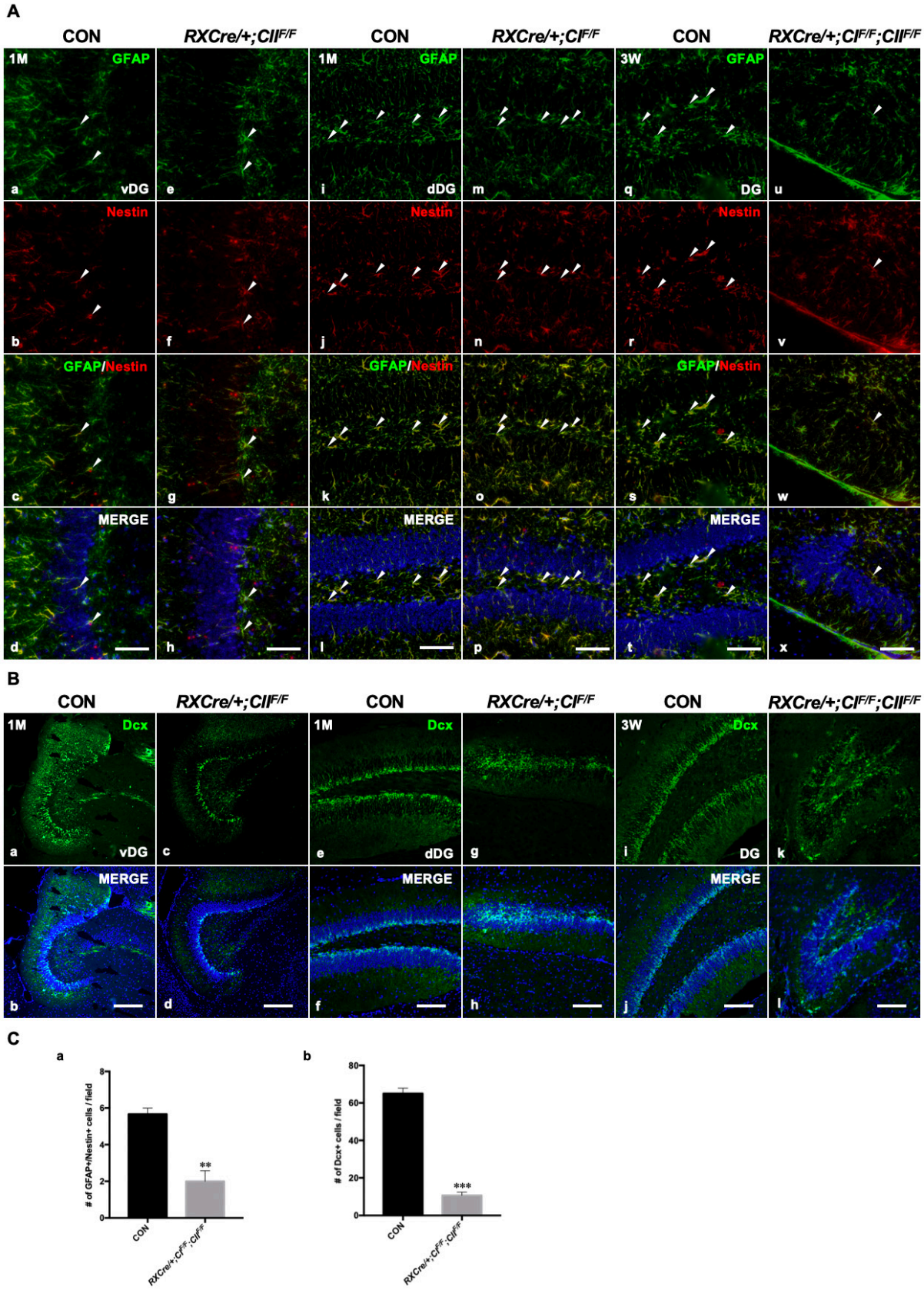

Figure 4, Yang et al.

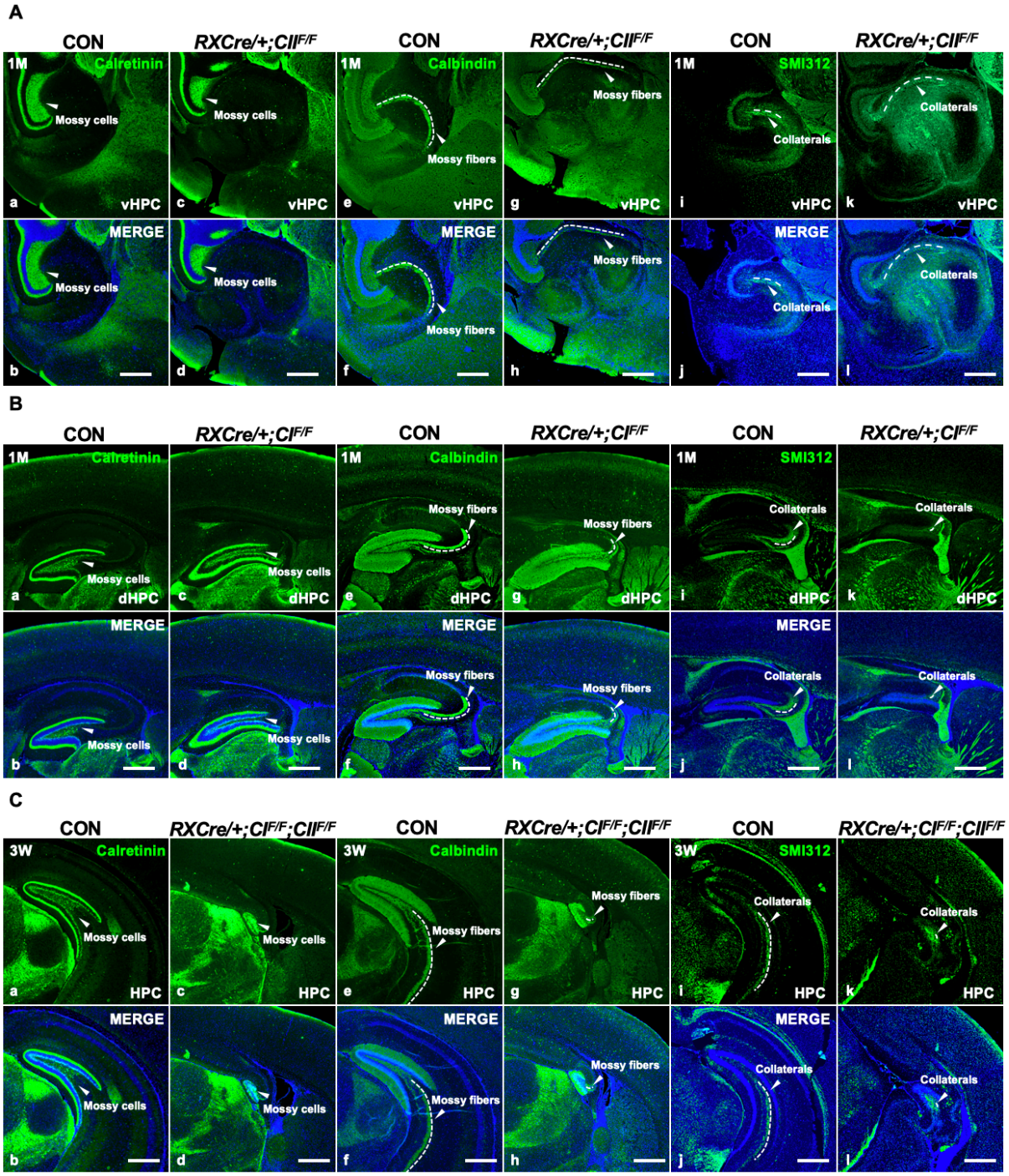

Figure 5, Yang et al.

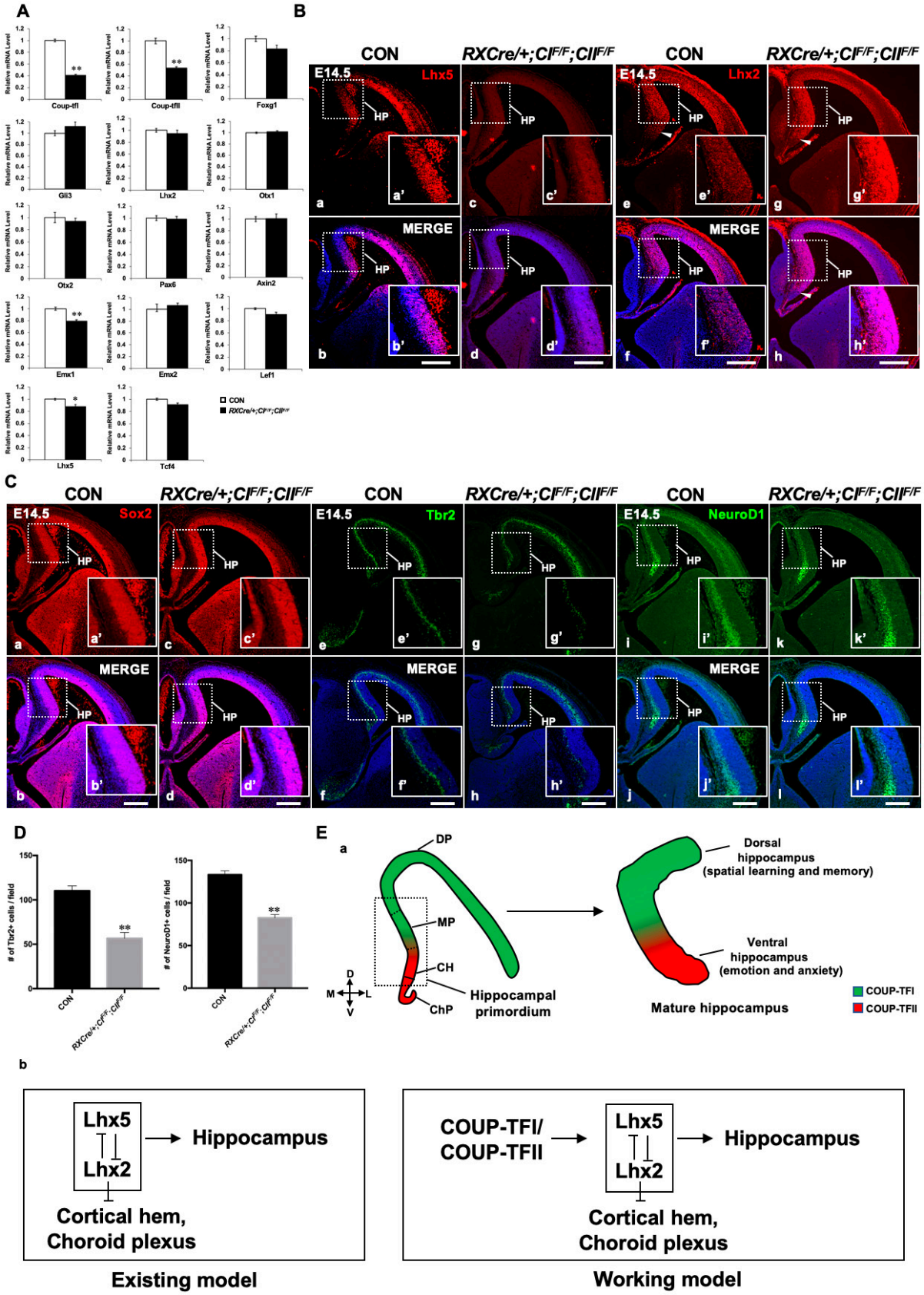
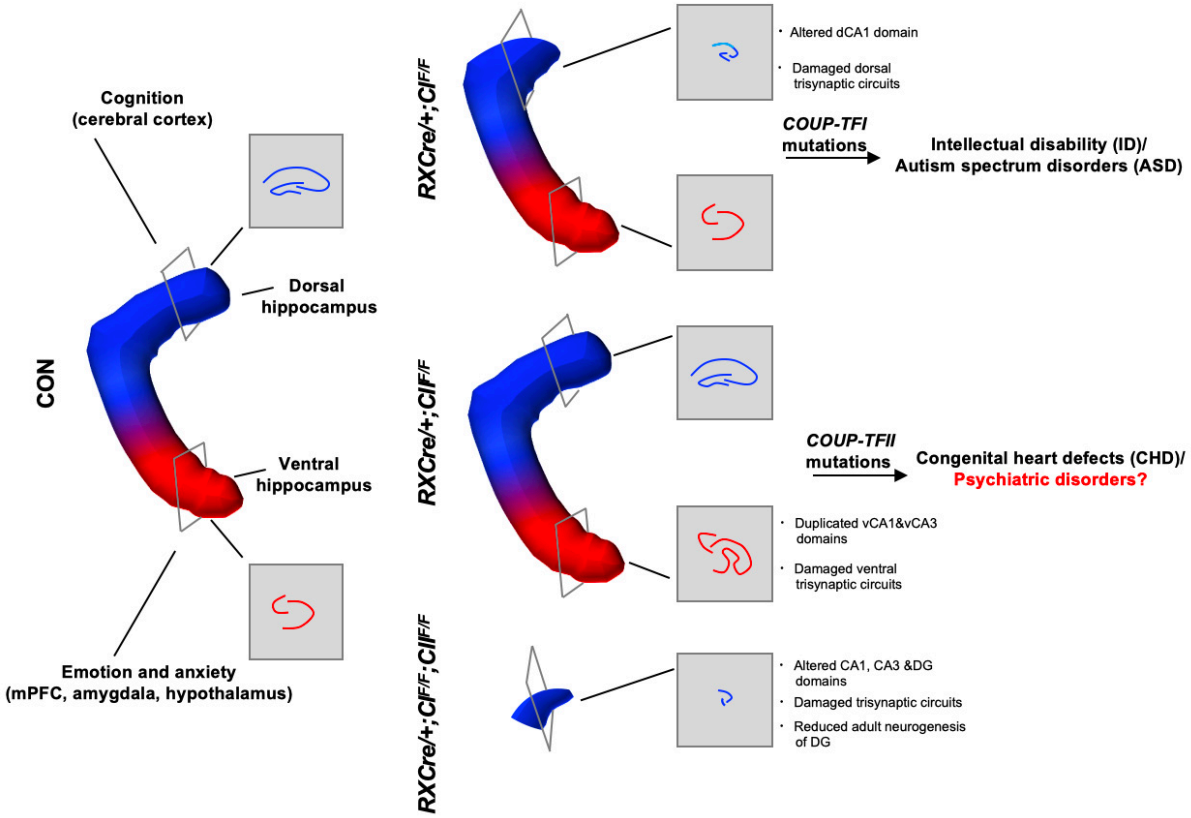
Figure 5—figure supplement 1, Yang et al.